Deep-Sea Research II 55 (2008) 2041–2058

Contents lists available at ScienceDirect

Deep-Sea Research II

journal homepage: www.elsevier.com/locate/dsr2

Sea ice in the western Antarctic Peninsula region: Spatio-temporal variability from ecological and climate change perspectives

Sharon E. Stammerjohn [a,b,*], Douglas G. Martinson [a,b], Raymond C. Smith [c,d], Richard A. Iannuzzi [a]

[a] Lamont-Doherty Earth Observatory of Columbia University, Palisades, NY 10964, USA
[b] Department of Earth and Environmental Sciences, Columbia University, New York, NY 10027, USA
[c] Institute for Computational Earth System Science, University of California, Santa Barbara, Santa Barbara, CA 93106, USA
[d] Department of Geography, University of California, Santa Barbara, Santa Barbara, CA 93106, USA

ARTICLE INFO

Article history:
Accepted 22 April 2008
Available online 24 July 2008

Keywords:
Antarctic zone
Antarctic Peninsula
Sea ice
Ocean–ice–atmosphere system
Climatic changes
Polar marine environment

ABSTRACT

The Antarctic Peninsula region is undergoing rapid change: a warming in winter of almost 6 °C since 1950, the loss of six ice shelves, the retreat of 87% of the marine glaciers, and decreases in winter sea-ice duration. Concurrently, there is evidence of ecosystem change along the western Antarctic Peninsula (wAP). Since the life histories of most polar marine species are synchronized with the seasonal cycle of sea ice, we assess how the seasonal sea-ice cycle is changing in the wAP region. Four new metrics of seasonal sea-ice variability were extracted from spatial maps of satellite derived daily sea-ice concentration: (a) day of advance, (b) day of retreat, (c) the total number of sea-ice days (between day of advance and retreat), and (d) the percent time sea-ice was present (or sea-ice persistence). The spatio-temporal variability describes distinct on-to-offshore and alongshore differences in ice–ocean marine habitats, characterized overall by a longer sea-ice season in coastal regions (6.8–7.9 months) versus a shorter sea-ice season over the shelf (4.1–5.3 months), with on-to-offshore differences increasing south-to-north. Large perturbations in the seasonality of the marine habitat occur in association with ENSO and Southern Annular Mode (SAM) variability. The local atmospheric response to these climate modes is largely a strengthening of the meridional winds during spring-to-autumn, which in turn affect the timing of the sea-ice retreat and subsequent advance. These perturbations are embedded in overall trends towards a later sea-ice advance, earlier retreat and consequently shorter sea-ice season, the impacts of which are expected to affect ecosystem functionality in the wAP region. A suite of ocean–atmosphere–ice interactions are described that are consistent with the amplified warming in late autumn, early winter.

Published by Elsevier Ltd.

1. Introduction

The seasonal and interannual variability of sea-ice affects many levels of the Antarctic marine ecosystem, from the timing and magnitude of seasonal primary production to the breeding success and survival of apex predators (Smith et al., 1995; Ross et al., 1996; Ducklow et al., 2007). This is consistent with the idea that the dominant influence causing variability in *marine* ecosystems is external physical forcing rather than internal biological mechanisms, which are the more dominant influences in *terrestrial* ecosystems (Steele, 1991). Therefore, understanding sea-ice variability, and the possible mechanisms influencing it, are essential aspects toward understanding changes in the polar marine ecosystem. This study evaluates seasonal sea-ice variability in the western Antarctic Peninsula (wAP) region, where there is strong evidence of rapid climate change over the last 50 years (Vaughan et al., 2003). Particular attention will be given to the area studied by the Palmer Antarctic Long-Term Ecological Research (PAL LTER) project (Fig. 1), which has conducted interdisciplinary research of the wAP marine ecosystem since 1990.

Passive microwave satellite remote sensing of polar oceans has provided continuous, full seasonal estimates of sea-ice concentration since 1979. These data are invaluable not only for characterizing sea-ice variability within the PAL LTER region but also for providing a longer and larger (Fig. 1) scale context for the PAL LTER. Previous studies of sea-ice variability in the PAL LTER region were based mostly on regional monthly averages of sea-ice coverage (Stammerjohn and Smith, 1996, 1997; Smith et al., 1998; Smith and Stammerjohn, 2001). Using these spatially averaged quantities, considerable variability in the annual cycle

* Corresponding author. Lamont-Doherty Earth Observatory, 61 Route 9W, Palisades, NY 10964, USA. Tel.: +1 845 365 8353; fax: +1 845 365 8736.
E-mail address: sharons@ldeo.columbia.edu (S.E. Stammerjohn).

0967-0645/$ - see front matter Published by Elsevier Ltd.
doi:10.1016/j.dsr2.2008.04.026

of seasonal sea-ice coverage in the PAL LTER region was revealed (Fig. 2). Over 1979–2004 the onset of the autumn sea-ice advance was as early as March or as late as May. Similarly, the termination of the spring retreat was as early as October or as late as March. Consequently, the duration of the sea-ice season was anywhere from 5 (1989) to 12 (1980) months.

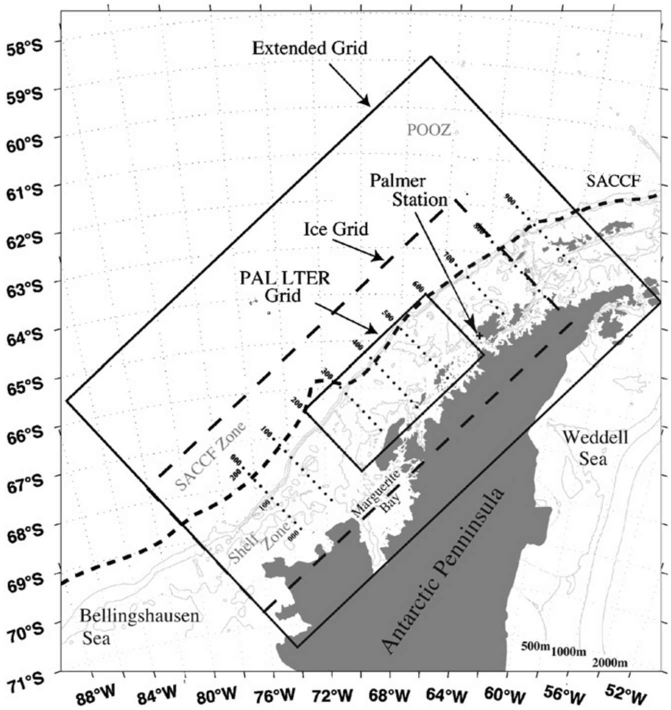

Fig. 1. Map showing the PAL LTER sampling area west of the Antarctic Peninsula with contoured bathymetry (gray lines at 500 m intervals). There are 10 nominal sampling lines, 100 km apart (numbered 000, 100, up to 900), and 11 sampling stations along each line, 20 km apart (numbered 000, 020, 040, up to 200). The dashed line labeled SACCF is the approximate location of the Southern Antarctic Circumpolar Current Front. In this paper we focus our attention on the spatio-temporal variability within the rectangular boxes labeled PAL LTER Grid (solid) and Ice Grid (dotted), the latter demarcating the minimum area that is fully covered by sea ice every year and therefore does not include the permanently open ocean zone (POOZ). The larger box (thin line) labeled the Extended Grid defines the area analyzed by Smith et al. (2008) in their study of SeaWiFS derived pigment biomass variability.

In addition to the high seasonal variability observed in the PAL LTER region, there also has been a strong and rapid warming of *winter* air temperature (almost a 6 °C increase since 1950) (King, 1994; King and Comiso, 2003; Vaughan et al., 2003), coincident with a trend towards decreased winter sea-ice *duration* in the wAP region (Smith and Stammerjohn, 2001; Vaughan et al., 2003; Parkinson, 2004; Stammerjohn et al., 2008). This is in contrast to weaker sea-ice trends observed elsewhere in the Southern Ocean except in the western Ross Sea, which shows strong *positive* trends in ice season duration (Yuan and Martinson, 2000; Parkinson, 2002; Liu et al., 2004; Stammerjohn et al., 2008). Stammerjohn et al. (2008) show that this decrease in the wAP sea-ice season is primarily due to a strong trend towards a later autumn advance and a somewhat weaker trend towards an earlier spring retreat (whereas in the western Ross Sea the increase in the ice season was due to trends towards an earlier advance and later retreat).

Coincident with the trend towards a shorter sea-ice season, there has been an increase in intra-seasonal variability between the 1980s and 1990s in the PAL LTER region (Fig. 2B). Sea-ice anomalies in the 1980s persisted longer, resulting in one to several years of positive anomalies followed by one to several years of negative anomalies. This several year oscillation in the 1980s was consistent with observations of an Antarctic Circumpolar Wave (ACW), which appeared to operate on a 7–8 year periodicity (White and Peterson, 1996). This behavior also made it easy to refer to a given year as a high or low ice year. In contrast, sea-ice anomalies in the 1990s often switched sign during a single sea-ice season, thus precluding the simple definition of high or low ice year (Smith et al., 1998; Stammerjohn et al., 2003). In general, there was much less persistence in the monthly sea-ice extent anomalies in the 1990s, and the 7–8 year oscillation was no longer readily apparent.

Throughout the South Pacific and western South Atlantic sectors of the Southern Ocean studies have shown strong co-variability between sea ice and El Niño Southern Oscillation (ENSO) (Simmonds and Jacka, 1995; Harangozo, 2000; Yuan and Martinson, 2000, 2001; Venegas et al., 2001; Kwok and Comiso, 2002; Meredith et al., 2004a; Turner, 2004; Yuan, 2004; Holland

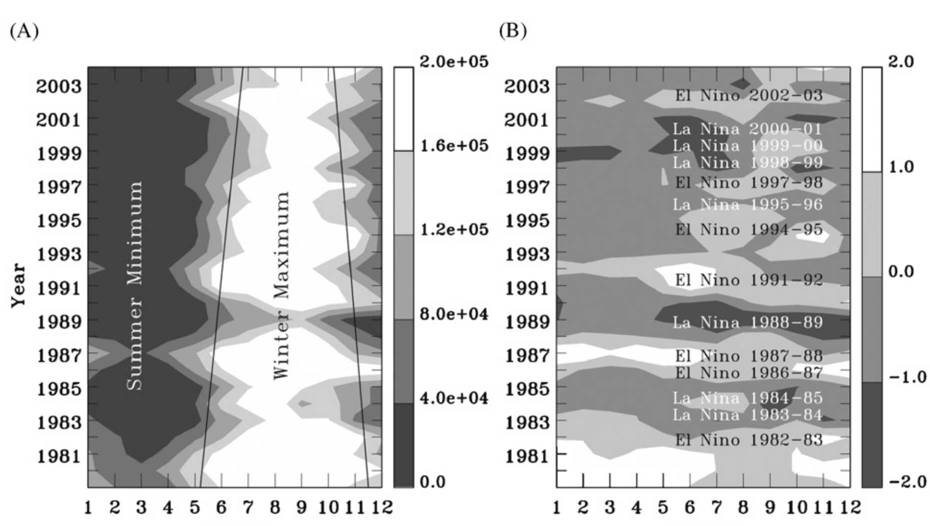

Fig. 2. (A) PAL LTER monthly sea-ice extent (km^2) and (B) monthly anomalies normalized by the standard deviation. In (A) the mean summer sea ice extent minimum (16,084 km^2) occurs in March, while the mean winter maximum (172,455 km^2) occurs in August. The trending lines show schematically that autumn sea-ice advance is occurring later with time, spring sea-ice retreat is occurring earlier with time, and both are creating a shorter winter ice season duration with time. In (B) ENSO years are defined according to the Climate Prediction Center (available from http://www.cpc.ncep.noaa.gov/products/analysis_monitoring/ensostuff/ensoyears.shtml).

et al., 2005; Lefebvre and Goosse, 2008). In general, positive sea-ice-extent anomalies in the PAL LTER region co-occur with El Niño events, while negative sea-ice-extent anomalies co-occur with La Niña events (Fig. 2B). There also is increasing evidence that the variability in the Southern Annular Mode (SAM), also known as the Antarctic Oscillation, is a strong influence on ocean–atmosphere–ice interactions in the wAP region (Hall and Visbeck, 2002; van den Broeke and Lipzig, 2003; Lefebvre et al., 2004; Liu et al., 2004; Meredith et al., 2004b, 2008; Lefebvre and Goosse, 2005; Marshall et al., 2006; Meredith and Hogg, 2006; Sen Gupta and England, 2006), particularly in the 1990s which saw a relatively high occurrence of the strong positive phase of SAM (Thompson et al., 2000; Thompson and Solomon, 2002; Marshall, 2003). Both ENSO- and SAM-related sea-ice variabilities in the wAP region will be further explored in this study.

Every austral summer since 1993, the PAL LTER has conducted research cruises in the wAP region (Fig. 1). In most years the PAL LTER region is free of sea ice in summer, but it may have just retreated several weeks, or several months, before the ship's arrival. The question then is how does ecosystem variability, as measured over a suite of physical–biogeochemical variables every summer, relate to the previous winter's sea ice cover? To begin examining this question, we needed to distill the seasonal information provided by the daily satellite data into ecologically meaningful yearly variables. As noted above, several components of the annual cycle of sea ice are believed to be ecologically relevant, which directed us to extract the following four sea-ice characteristics from the daily maps of sea-ice concentration: (a) the day of sea-ice advance, (b) the day of sea-ice retreat, (c) the total number of days sea ice was present (or total sea-ice days), and (d) the percent time sea ice was present (sea-ice persistence) during the defined winter period. With these four sea-ice characteristics the key components of the annual cycle of sea ice were mapped for the wAP region, showing geographically where sea ice arrived and departed earlier or later, where it persisted longer, or came and went throughout the winter period.

In this paper our primary focus is to examine sea-ice variability from 1992 to 2004 so that it can be related to *in situ* data collected within the PAL LTER program. However, given the changes we noted in reference to Fig. 2, we also will compare this time period to changes that occurred over the longer (1979–2004) satellite period and over the greater wAP region. There are four hydrographic and biogeochemical subdivisions in the wAP region based on the delineations of major frontal systems that control nutrient dynamics and hence phytoplankton production (Tréguer and Jacques, 1992): (1) a highly productive Coastal and Continental Shelf Zone (CCSZ), (2) a relatively productive Seasonal Ice Zone (SIZ, that area annually covered by sea ice), (3) a highly but intermittently productive zone within the SIZ that lies over the area of the Southern Antarctic Circumpolar Current Front (SACCF) just offshore of the shelf break, and (4) a less productive Permanently Open Ocean Zone (POOZ). For the sea-ice analyses, we define a sea-ice grid (Fig. 1), which delineates the minimum area covered by sea ice every year of 1992–2004, thus it does not include the POOZ but does include the other three subdivisions. Additionally, Smith et al. (2008) discusses all four of these hydrographic and biogeochemical subdivisions in the wAP region within the context of satellite derived phytoplankton biomass, winds and sea ice.

2. Data and methods

Satellite measurements of sea-ice concentration are from NASA's Scanning Multichannel Microwave Radiometer (SMMR) and the Defense Meteorological Satellite Program's (DMSP) Special Sensor Microwave/Imager (SSM/I). Sea-ice concentrations were determined using the Bootstrap passive microwave algorithm (Comiso, 1995; Comiso, 2003), from which an SMMR-SSM/I time series was created that minimizes the differences between the various SMMR and SSM/I sensors (Comiso et al., 1997). This study uses the every-other-day SMMR and the daily SSM/I time series (1979–2004) as well as the monthly averaged data as provided by the EOS Distributed Active Archive Center (DAAC) at the National Snow and Ice Data Center, University of Colorado in Boulder, Colorado (http://nsidc.org). The sea-ice concentration data are mapped to a 25 25-km grid on a polar stereographic projection and include a landmask and latitude/longitude pairs for geolocating pixels.

Four sea ice characteristics (day of advance, day of retreat, ice days, and ice persistence) were determined from the (quasi) daily images of SMMR-SSM/I sea ice data. The year days of advance and retreat were determined at each grid point for each sea-ice year (defined here to begin and end at the mean summer sea-ice extent minimum as observed in the PAL LTER region: March 15 of current year to March 14 of following year). When sea-ice concentration increased past 15% (or for comparison, 50%) and remained above that threshold for at least 5 days, then the day of advance was identified as the first day of that 5-day sequence. Day of retreat was similarly defined as the last day of the sea-ice season that sea-ice concentration was above the given threshold for at least 5 consecutive days. If sea-ice concentration never decreased below the given threshold for the year in question (i.e. remained annually ice covered at that threshold), then day of advance and retreat were set to the lower (March 15) and upper limits (March 14 of following year), respectively. If sea-ice concentration never exceeded the given threshold for at least 5 days, then all four sea-ice variables were set to zero, i.e. the value for open ocean.

Ice days are the number of days between day of advance and day of retreat when sea-ice concentration exceeded the given threshold. The number of sea-ice days can be less than the interval between day of advance and retreat if (1) the ice-edge advanced then retreated in an oscillatory fashion (usually during the autumn advance or spring retreat), or (2) openings occurred within the pack ice during periods of divergence (e.g., by winds, tides, currents). This difference is captured by the last sea-ice characteristic, sea-ice persistence, which is the percent time sea ice is present within the interval between day of advance and retreat.

The sea-ice characteristics were processed on the original satellite polar stereographic grid (25 km by 25 km), then re-mapped into the Ice and PAL LTER grids. The Ice grid has a cell size of 50 km (on-to-offshore) by 100 km (along-shore), while the PAL LTER grid has a cell size of 40 km (on-to-offshore) by 100 km (along-shore). Given the higher resolution and different projection of the satellite data, 5–8 satellite observations per year were binned into each Ice and PAL LTER grid cell and averaged. Although the sea-ice characteristics are derived from daily satellite data, the extracted information (e.g., day of advance) represents just one yearly value per grid cell for a total of 13 years of data (1992–2004). We present spatial maps of both the climatology and yearly anomalies, which show, for each grid cell, the 13-year mean and yearly departure from the 13-year mean, respectively.

Further quantification and insight into the interannual variability and its spatial structure is obtained via classical Principal Component Analysis (PCA), which decomposes the data into orthogonal modes. The spatial structure of these modes is contained in the empirical orthogonal function (EOF), which is calculated from the sample covariance matrix, where the lower order EOFs represent spatially-coherent structures whose shapes are preserved through time. The time-varying amplitudes of these shapes (the full modal structure of the EOFs) are then calculated; these are the principal components (PCs). Martinson et al. (2008) give further details of the PCA analysis employed on the PAL LTER data. Here we show only the first (gravest) mode, which describes the largest amount of the data variance.

In this study we also compared sea-ice variability to ENSO and SAM variability. The ENSO index used is the Niño 3.4 sea-surface temperature index consisting of averaged eastern equatorial Pacific sea-surface temperature for 5°N–5°S, 170–120°W (Cane et al., 1986) (available at http://iridl.ldeo.columbia.edu/docfind/databrief/cat-index.html). However, we also compared our results to the Southern Oscillation Index (SOI) that consists of the difference between the standardized sea-level pressures (SLPs) at Tahiti and Darwin (available at the IRI website given above). In general, we obtain similar results when using either the Niño3.4 or SOI index. The SAM index used here is an observation-based index provided by Gareth Marshall (available at http://www.nerc-bas.ac.uk/icd/gjma/sam.html) (Marshall, 2003). We also use 10-m wind and SLP data (1990–2004) of the wAP region extracted from numerically analyzed data of the National Center of Environmental Prediction and National Center for Atmospheric Research Reanalysis (NNR) Project (Kalnay et al., 1996).

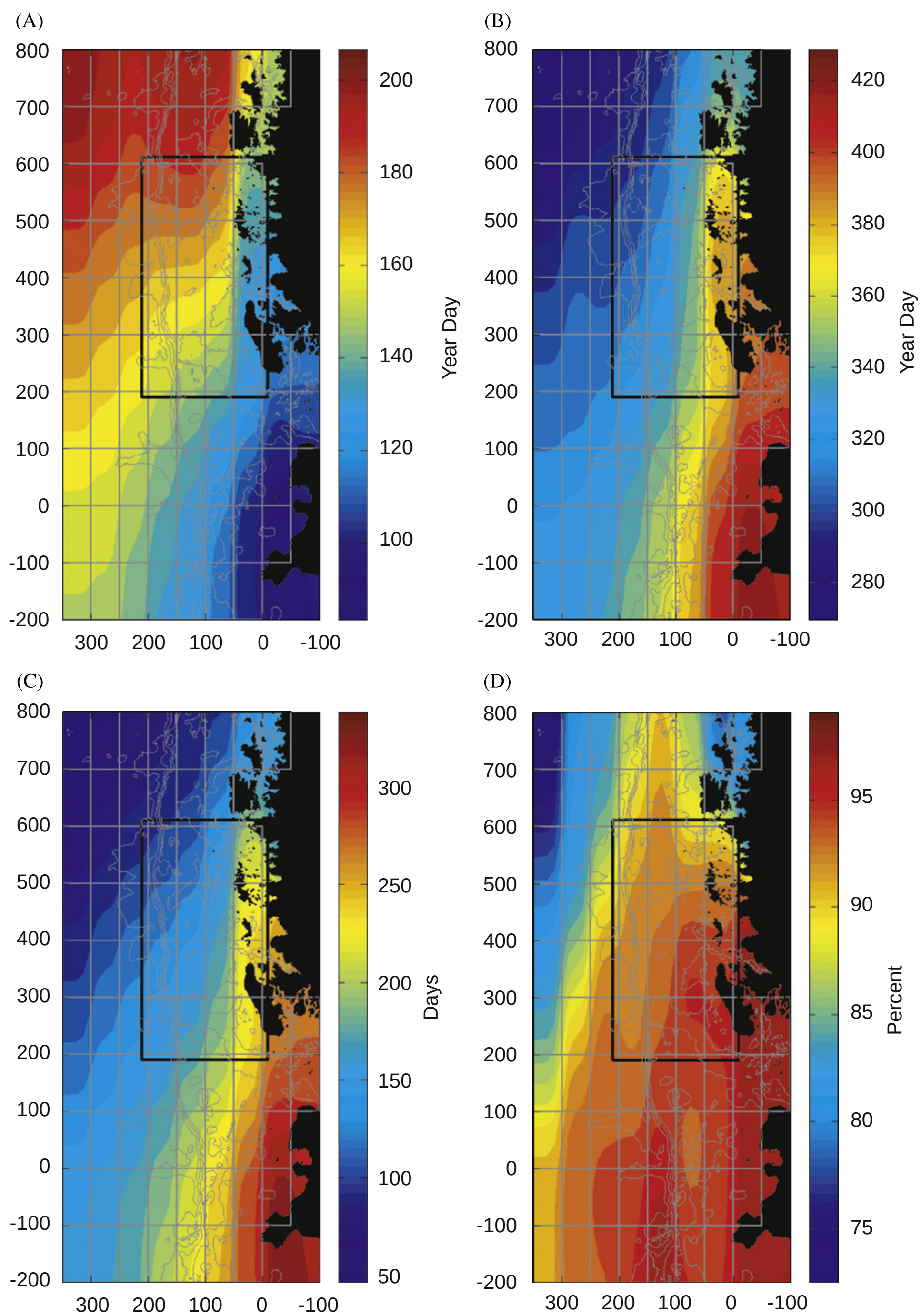

Fig. 3. Spatial climatology maps of (A) day of advance (year day), (B) day of retreat (year day), (C) ice days (total days) and (D) ice persistence (%). The black box outlines the PAL LTER Grid, and bathymetry is contoured (in gray) at 500, 1000, 2000 and 3000 m depth levels. Grid cells are in gray (50 × 100 km); where there are no grid cells (e.g., lower right corner, around land), values are spatially interpolated.

3. Results

3.1. Mean and temporally varying seasonal sea-ice patterns

The 1992–2004 climatologies of the four sea-ice characteristics within the wAP region show both strong on-to-offshore and along-shore differences (Fig. 3). Sea-ice advance is earlier and retreat later both inshore and south compared to offshore and north, and these differences in the timing of advance and retreat manifest as a longer sea-ice season in coastal areas versus a shorter sea season over the shelf, again with on-to-offshore differences increasing northward. For example, in the northern part of the PAL LTER area the on-to-offshore difference in the timing of ice advance is about 2.6 months, retreat about 3.5 months, thus explaining the approximate 6.1 month difference in the number of ice days on-to-offshore. This is in contrast to an on-to-offshore difference in the number of ice days of only 2.5 months for the southern part of the grid.

The coastal regions within the PAL LTER area are further distinguished by varying sea-ice persistence (Fig. 3D) and overall year-to-year variability. Despite a relatively long sea-ice season in the northern coastal region (i.e. the Palmer Basin area inshore of the 500 and 600 lines), there is lower sea-ice persistence here, indicating frequent openings of the sea-ice cover, as well as higher year-to-year variability. This is in contrast to high persistence and low variability observed elsewhere along the coast. We also examined the timing of sea-ice advance and retreat at concentrations greater than 50% (not shown) as an indicator of the arrival of more consolidated pack ice conditions. The temporal lag, between when the ice edge first arrived, and when consolidated ice conditions next appeared, was greatest in the northern and central (i.e. inshore of the 400 line) coastal regions within the PAL LTER area. Thus, the longer sea-ice season in the northern and central coastal regions was due to a longer duration of low (15–50%) sea ice concentration. In contrast, the southern coastal region within the PAL LTER area (i.e. Marguerite Bay vicinity inshore of the 200 and 300 lines) shows the highest sea-ice persistence and the longest sea ice season with concentrations greater than 50% (relative to the rest of the PAL LTER area).

The 13 yearly anomalies for day of advance, day of retreat, and ice days (Fig. 4) illustrate spatially the year-to-year variability about the climatology. The most notable anomalies within the PAL LTER grid for day of advance (Fig. 4A) are the two strong negative anomalies in 1992 and 2002 (indicating early autumn advances) and the three consecutive large positive anomalies from 1999 to 2001 (indicating late autumn advances). In general, there seems to be a grid-wide temporal shift from mostly negative anomalies in 1992–1997 to mostly positive anomalies from 1998 to 2001 (i.e. a shift towards a later autumn advance). Martinson et al. (2008) also report similar temporal shifts in upper ocean bulk properties. In contrast, the yearly anomalies for day of retreat (Fig. 4B) show no indications of a temporal grid-wide shift and in general show more variability. The yearly anomalies for ice

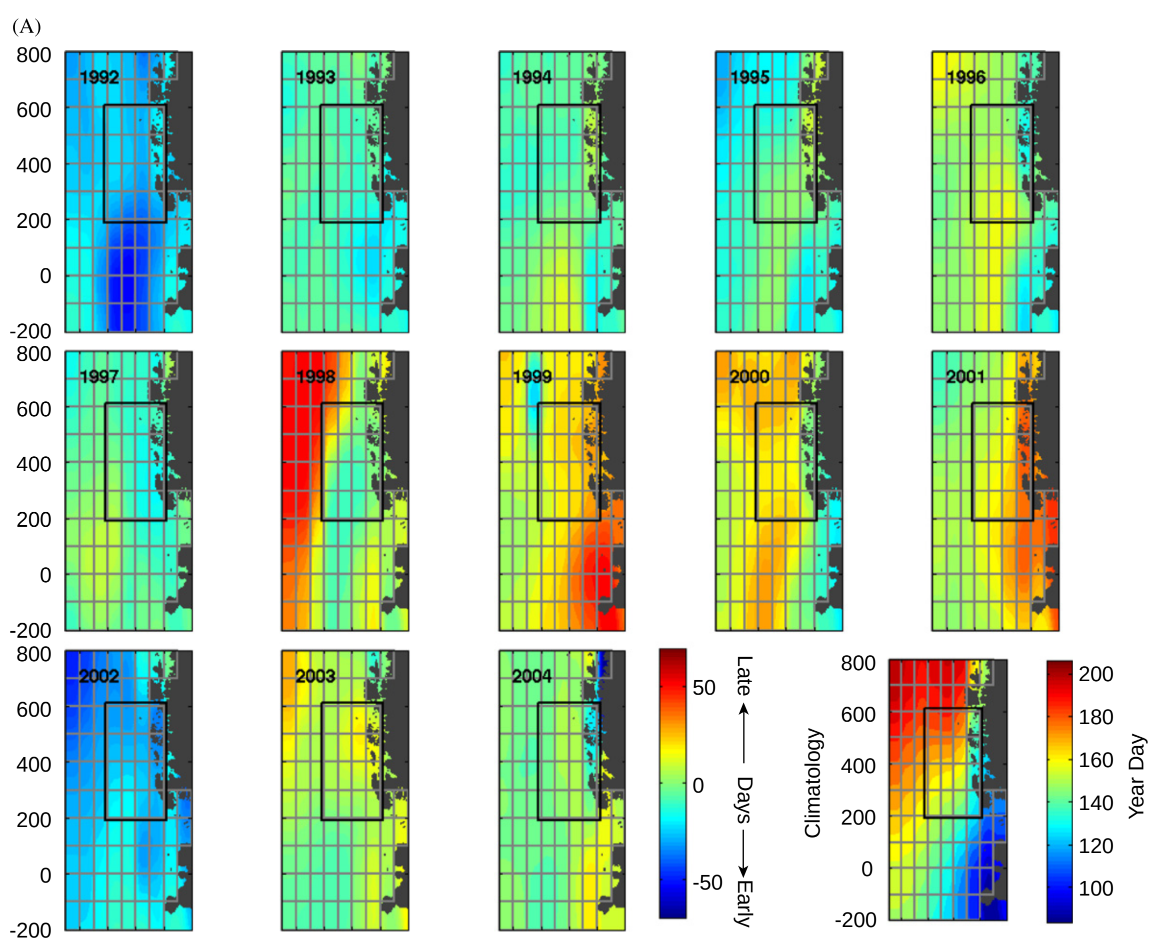

Fig. 4. Spatial anomaly maps for (A) day of advance, (B) day of retreat, and (C) ice days. The black box outlines the PAL LTER Grid. For day of retreat (B) the positive (red) anomaly in the 1998 map (left edge, middle) traces an iceberg track. The iceberg trace is still visible in the subsequent 1999 advance (A), seen as the negative (blue) anomaly upper left. Grid cells are in gray (50 100 km); where there are no grid cells (e.g., lower right corner, around land), values are spatially interpolated.

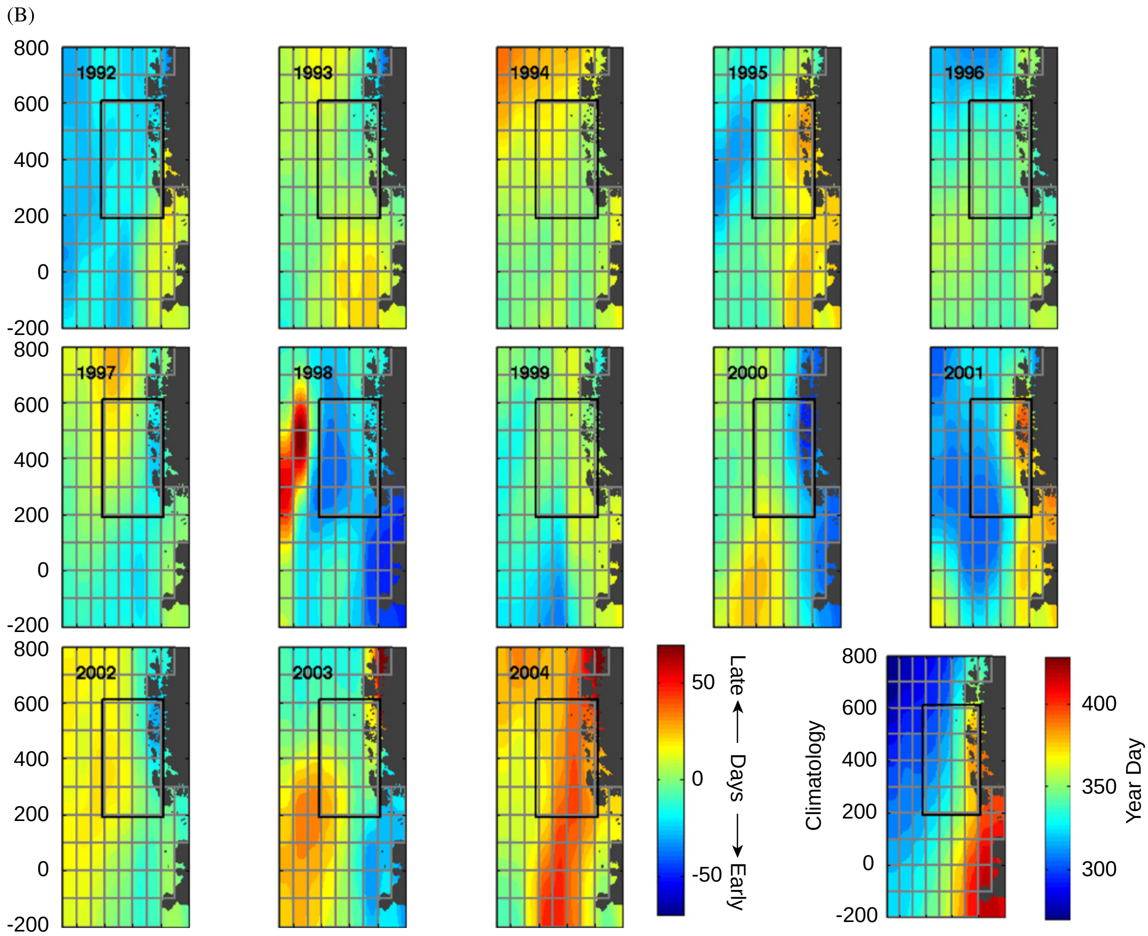

Fig. 4. (*Continued*)

days (Fig. 4C) integrate the anomalies in both advance and retreat, and like the yearly anomalies for day of advance, there is an indication of a temporal grid-wide shift, illustrated here as a shift to strong negative anomalies (fewer ice days) from 1998 to 2001. The timing of this shift appears to begin in the autumn of 1998 and ends, or is interrupted, in the summer of 2002. (Since our time series goes only to 2004, there is no way to assess whether this shift is long term or not.) This grid-wide temporal shift, as well as the rapid shifts from high to low (1997–1998) and low to high (2001–2002) sea-ice conditions, will be discussed further in Section 3.3 within the context of ENSO and SAM variability.

The dominant spatio-temporal sea ice anomaly patterns revealed in the first PCA mode (Fig. 5) spatially distill the observed sea-ice variability over 13 years (Fig. 4), and depending on the sea-ice characteristic, the first PCA mode explains 47–70% of the overall temporal variance. Thus, the maps of the first EOF show the most frequently occurring spatial anomaly patterns that vary year-to-year according to the PC time series. For example, year 1998 had the highest negative PC value for ice days, and in conjunction with the EOF anomaly map, was characterized by high negative anomalies offshore but only moderately negative anomalies inshore (relative to offshore), while year 2002 had high positive anomalies offshore but again only moderately positive anomalies inshore. In general, the PC time series indicate high variability during 1998–2002 and 2004 as compared to other years. Spatially, the maps of the first EOF for sea-ice retreat, ice days and ice persistence show similar on-to-offshore patterns, with highest variability over the shelf, less variability near the coast. In contrast, the map of the first EOF for advance is distinctly different showing highest variability mid-shelf in the northern part of the PAL LTER grid and in the south coastal region (i.e. Marguerite Bay vicinity).

For the PAL LTER region and for the Southern Ocean as a whole, there is little temporal co-variability between the autumn sea-ice advance and the spring sea-ice retreat, indicating that anomalies are not coherently generated over the autumn-to-spring (i.e. over winter) period (Stammerjohn et al., 2008). In contrast, there is more co-variability between the spring sea-ice retreat and subsequent autumn sea ice advance, indicating that more often than not, temporally coherent anomalies are generated over the spring-to-autumn (i.e. over summer) period. Also there is more spatial coherency on-to-offshore in the autumn sea-ice advance than there is in the spring sea-ice retreat. This may in part be due to the fact that the equatorward expansion of sea ice during advance is unconstrained physically (no continental boundary to the immediate north), thus is able to respond coherently to cooling air temperatures from south to north as the autumn season progresses into winter. In addition, sea-ice advance (more so than sea-ice retreat) is sensitive to rapid changes in atmospheric conditions given the ability to rapidly vent ocean heat, especially during cold air outbursts. In contrast, the spring sea-ice retreat is constrained both physically by the Antarctic continent, and by increasing sea-ice thickness to the south. Finally, the temporal variability in sea-ice advance, more so than sea-ice retreat, is more strongly correlated to temporal variability in ice

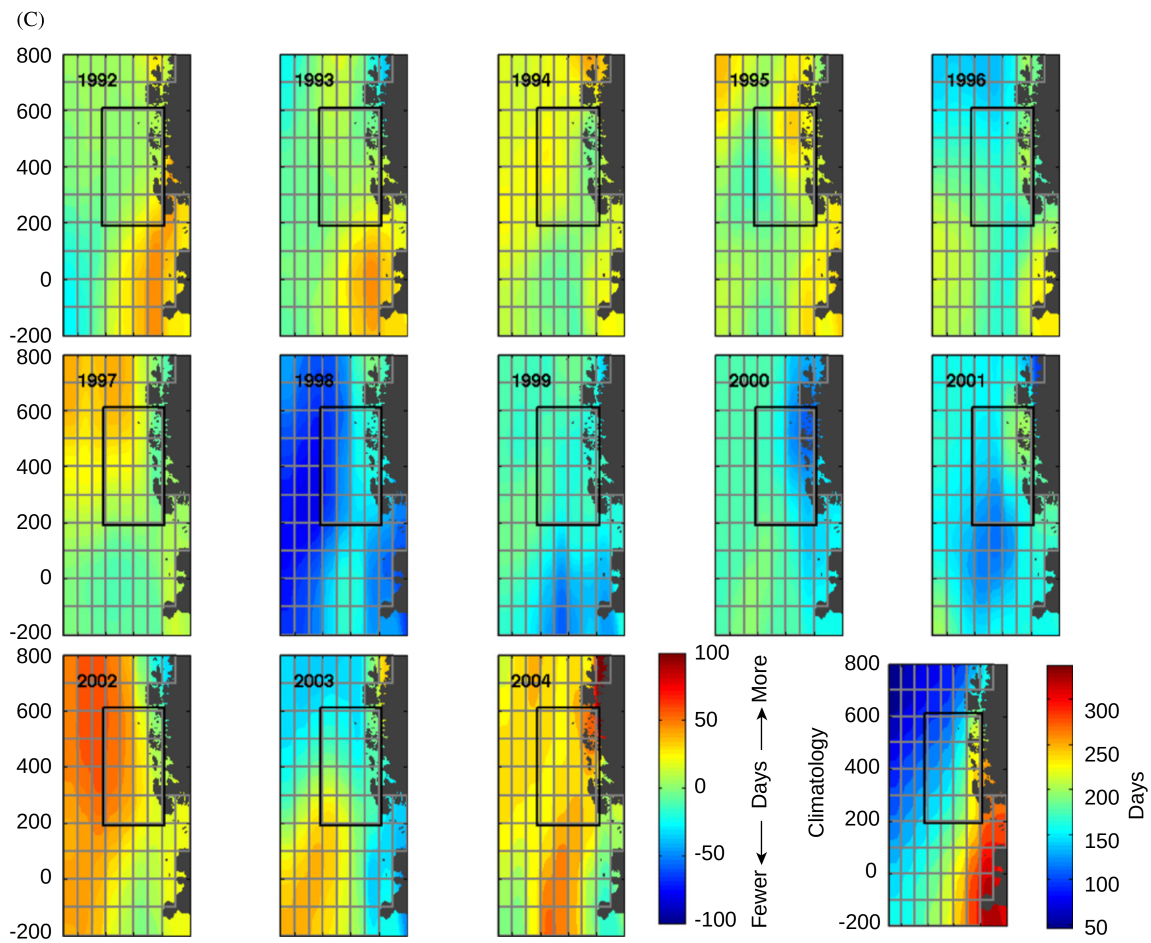

Fig. 4. (*Continued*)

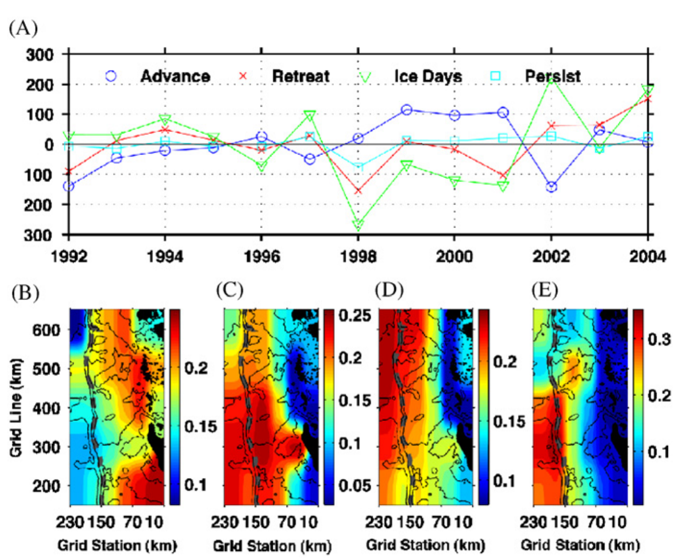

Fig. 5. (A, top) The time expansion coefficients (1992–2004) of the first principal component (PC) shown for the four sea-ice characteristics for the PAL LTER Grid, and (bottom) the individual spatial EOF maps for (B) day of advance, (C) day of retreat, (D) ice days and (E) ice persistence, where the thick dashed line demarcates the shelf break. Percent variance explained by the first mode is in (B) 64.4%, (C) 46.8%, (D) 69.2%, and (E) 58.6%.

days (Stammerjohn et al., 2008). As will be shown in Sections 3.3 and 3.4, the temporal variability in sea-ice advance appears to more clearly capture climate signals given its sensitivity to ocean–atmospheric variability and its free unconstrained expansion.

3.2. *Seasonal ice– ocean co-variability*

The melting of sea ice every spring constitutes a cold (1.8 °C), freshwater (6 ppt, average sea ice salinity) input into the ocean surface mixed-layer. It therefore follows that the variability in sea-ice has some influence on the salt and heat content of the upper ocean summer mixed layer. To test these relationships, we use two summer mixed layer ocean bulk properties defined and described by Martinson and Iannuzzi (1998) and Martinson et al. (2008): (1) the seasonal salt deficit (SDS), whereby a positive SDS anomaly indicates a larger volume of freshwater content (i.e. larger salt deficit) relative to the higher salinity waters below, and (2) the seasonal thermal barrier (TBS), whereby a positive TBS anomaly indicates higher heat content, thus a stronger barrier to the cold waters below. In general, there is higher salt (lower SDS, Fig. 6A) and heat content (higher TBS, Fig. 6C) offshore versus inshore, together with deeper mixed layers (not shown, however the spatial pattern is very similar to the TBS climatology). Along the coast, there are distinct relative differences: the northern coastal region shows higher salt but lower heat content and shallower mixed layers, while the southern coastal region shows lower salt (high SDS) but higher heat content and deeper mixed layers.

Throughout most of the PAL LTER area the temporal variability in SDS co-varied most strongly and widely with the previous

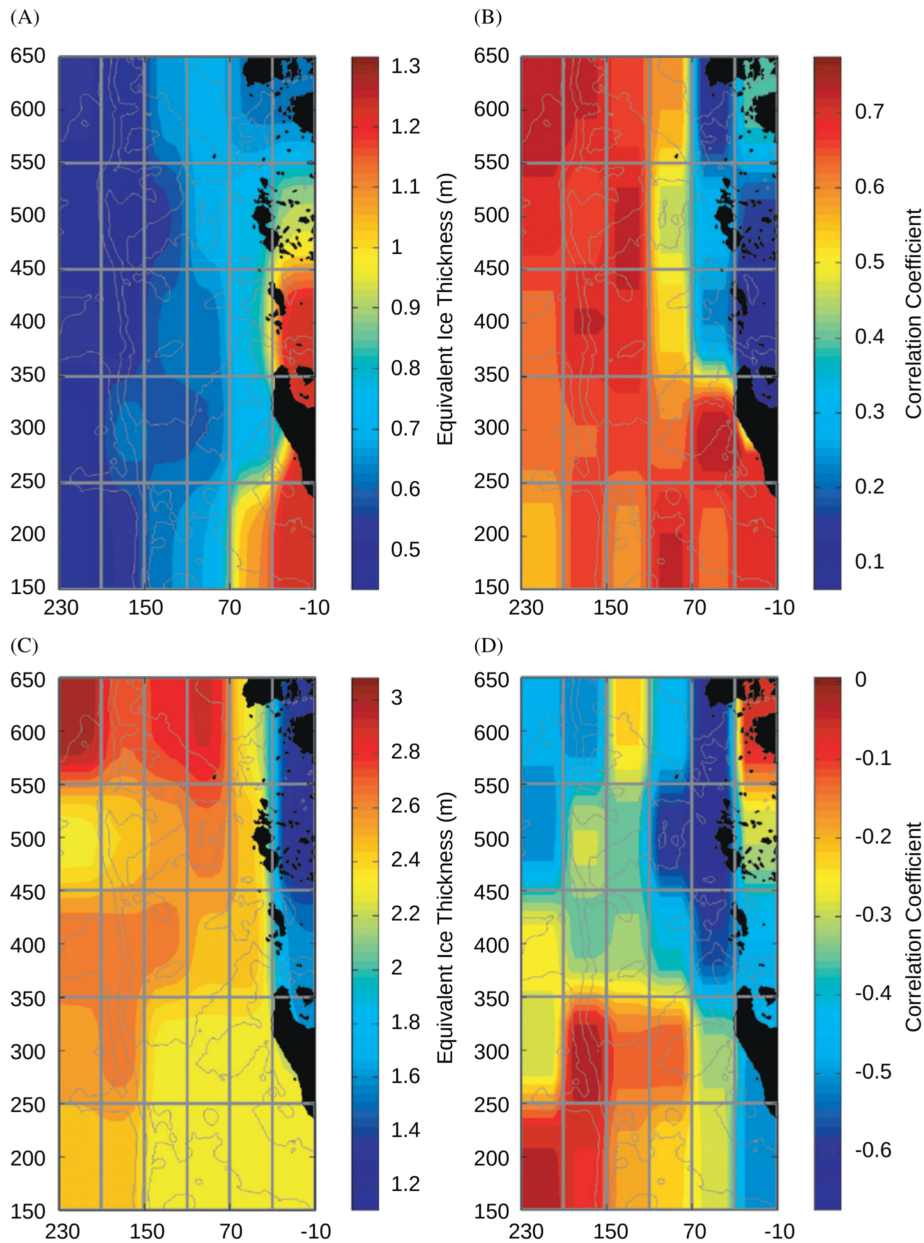

Fig. 6. (A) Spatial climatology map of seasonal salt deficit (SDS) in units of equivalent ice thickness; (B) correlation map of SDS versus the number of ice days the previous winter (orange-reds indicate strong positive correlation); (C) spatial climatology map of seasonal thermal barrier (TBS) in units of equivalent ice thickness; and (D) correlation map of TBS versus day of retreat (at 50% threshold) the previous spring (blues indicate strong negative correlation). Units of equivalent ice thickness indicate the thickness (in meters) of *in situ* ice growth required to eliminate the seasonal salt deficit, or thermal barrier, relative to the underlying waters (see Martinson et al., 2008, for further details). In gray are rectangular grid cells (40 100 km) and bathymetry contoured at 450, 1500 and 3000 m depth levels.

winter's number of ice days (Fig. 6B), whereby higher SDS (greater freshwater content) was associated with a longer sea-ice season in the previous winter. The exceptions are the northern and central coastal regions and to a lesser degree the southern shelf break region (which becomes a more obvious exception when tracking sea-ice concentrations at the 50% threshold). Additional observations indicate that the northern coastal region is strongly influenced by glacial meltwater input (Dierssen et al., 2002), while the southern shelf break region is most susceptible to intrusions of (salty) upper Circumpolar Deep Water (UCDW) (Martinson et al., 2008). Outside these regional exceptions, the high correlation between SDS and ice days indicates that the melting of sea ice is the dominant contributor determining the salt content, such that the other processes influencing seasonal mixed layer properties (e.g., precipitation, cross-pycnal mixing) are not large enough in magnitude to significantly change the seasonal salt content established by the ablation of the previous winter's sea-ice cover (see also Martinson, 1990). The strong relationship between SDS and ice days also infers that the number of ice days can serve as a proxy for ice volume: a longer (shorter) ice-covered period infers thicker (thinner) sea ice (via both thermodynamic and mechanical thickening processes), and thicker (thinner) *in situ* sea-ice melt is associated with higher (lower) SDS, i.e. freshwater content.

The temporal variability in seasonal mixed-layer heat content (TBS) was most related to surface air temperature variability in spring–summer, which in turn generally co-varied with the timing of sea ice retreat (though not always; see Section 3.4). Thus, lower

TBS (i.e. colder seasonal mixed layer; negative anomaly) was often associated with a later spring sea-ice retreat (positive anomaly) and vice-versa, resulting in negative co-variability between TBS and sea-ice retreat (Fig. 6D). Or, in other words, the shorter (longer) the time between when sea ice retreated and TBS was measured (in Jan–Feb), the less (more) time to warm by insolation. This relationship was strongest for sea-ice retreat at the 50% sea-ice concentration threshold (Fig. 6D) versus the 15% threshold (not shown), indicating that heating by insolation already begins when the pack ice first starts to break up. In addition, the strongest correlations are found mid-shelf in the northern half of the grid and in the coastal region of the southern half of the grid. Thus, the regional exceptions (north coast, south shelf break) are similar to those observed between SDS and ice days, though different in their spatial extent (e.g., low correlations in the south shelf break region extend to mid-shelf).

In summary, the main on-to-offshore, and alongshore, seasonal ice–ocean patterns are described for the PAL LTER region (Table 1) by distinguishing two sub-regions over the shelf (north and south) and three along the coast (north, central and south). A sixth sub-region, lying offshore of the shelf break, also is described for regional context and is further discussed by Smith et al. (2008) who show this region to be influenced by the SACCF. Mean statistics for each of the five PAL LTER sub-regions are provided as Supplementary Online Material (Table S1).

In general, the north coast sub-region is distinguished by a long season of low sea-ice concentration, as well as frequent openings and closings of the sea-ice cover. In turn, this high variability in sea ice of low concentration is related to high variability in heat content (high TBS): the variable sea-ice conditions create a highly variable upper ocean light environment and thus variable heating by insolation. Low sea-ice concentration also indicates that freshwater input from sea-ice melt is minimal here (relative to the other coastal regions). As mentioned above, this area is strongly influenced by glacial meltwater input (Dierssen et al., 2002), examples of which are the summers of 1997, 1998 and 2001 when the previous winter's ice days were low (Fig. 4C), but freshwater content in the summer surface mixed layer was high (high SDS) (Martinson et al., 2008). These same summers showed very warm air temperature, which would have contributed to significant amounts of glacial meltwater input, thus contributing to the high freshwater content. These inferences of a glacial meltwater influence are supported by analyses of water chemistry (Carrillo, pers. comm.) and water turbidity (Dierssen et al., 2002).

The central coast sub-region is distinguished by numerous archipelagos and by a long, persistent sea-ice season. The islands appear to aid and abet the retention of both sea ice and freshwater ice (e.g., icebergs and brash ice). The characteristically high mixed layer freshwater content is therefore the result of large volumes of ice melting *in situ*, with potentially large, but varying, contributions from freshwater ice. Spatial variability in mixed-layer heat and salt content also shows this region to be a transition zone between the high variability in heat content in the north coast sub-region and the high variability in salt content in the south coast sub-region.

The south coast sub-region is distinguished by being the entrance to Marguerite Bay. It also is distinguished by having the highest mixed-layer freshwater content across the grid, indicating large volumes of sea-ice melting *in situ*. Indeed, the mean number of ice days (greater than 50% sea ice concentration) and sea ice persistence are highest here. Glacial meltwater contributions, though likely present, especially during warm summers, appear to be minimal relative to the contribution from *in situ* ice melt.

The north and south shelf regions are generally characterized by high mixed layer heat and salt content, high correlations

Table 1
Summary of mean (1992–2004) ice-ocean characteristics for five sub-regions within the PAL LTER area, as well as for the area just offshore of the PAL LTER

Line k	Offshore of shelf	Shelf	Coast
600	*North– South (200– 600 lines)*	*North (400– 600 lines)*	*North (500– 600 lines)*
	1. Late advance (6/23)	1. Latest advance (6/28)	1. Early advance (5/20)
	2. Earliest retreat (11/2)	2. Early retreat (11/9)	2. Late retreat (1/16)
500	3. Shortest ice season (3.8)	3. Short ice season (4.1)	3. Long ice season (7.3)
	4. Short consolidated (3.3)	4. Short consolidated (3.3)	4. Moderate consolidated (4.1)
	5. SACCF influence	5. Frequent opening/closing	5. Frequent opening/closing
		6. High salt and heat content	6. Moderate salt and heat content
			7. Glacial meltwater influence
400			*Central (400 line)*
			1. Early advance (5/19)
			2. Latest retreat (1/24)
			3. Longest ice season (7.9)
			4. Long consolidated (5.5)
			5. Moderate opening/closing
			6. Low salt and heat content
			7. Glacial meltwater influence
300		*South (200– 300 lines)*	*South (200– 300 lines)*
		1. Moderate advance (6/5)	1. Early advance (5/24)
		2. Early retreat (11/23)	2. Moderate retreat (12/25)
		3. Moderate ice season (5.3)	3. Long ice season (6.8)
		4. Moderate consolidated (4.7)	4. Longest consolidated (5.9)
200		5. Moderate opening/closing	5. Few opening/closing
		6. High salt and heat content	6. Low salt, moderate heat content
		7. UCDW influence	7. Large in situ sea ice melt
Station-	350–200	200–070	070–000

Relative qualifiers highlight sub-regional differences. Mean days of advance/retreat are given as month/day, and mean ice days are given in decimal month. Consolidated refers to portion of ice season with concentrations greater than 50% (in decimal months). Opening/closing refers to opening/closing of pack ice after initial ice-edge advance and before final retreat. Salt and heat content refer to integrative quantities of the summer surface mixed layer (see Martinson et al., 2008). SACCF: Southern Antarctic Circumpolar Current Front; UCDW: Upper Circumpolar Deep Water.

between summer salt content and previous winter's number of ice days, and low variability in summer surface mixed layer properties. The south shelf region is distinguished from the north by a longer sea-ice season and evidence of frequent intrusions of UCDW (Martinson et al., 2008). Finally, the region offshore of the shelf break is distinguished by having the shortest sea-ice season (relative to the PAL LTER area), low sea-ice persistence and evidence of an SACCF influence (Smith et al., 2008).

3.3. ENSO- and SAM-related ice-atmosphere anomalies

Atmospheric circulation variability in the wAP region is strongly influenced by both ENSO and SAM variability (references given in Introduction). The high-latitude ENSO response in the South Pacific sector of the Southern Ocean is characterized by positive pressure anomalies roughly between 60–70°S and 90–130°W (i.e. upstream of the wAP region) during El Niño and negative pressure anomalies during La Niña (e.g. Yuan, 2004; Lachlan-Cope and Connolley, 2006; Meredith et al., 2008). SAM variability is characterized by zonally symmetric atmospheric pressure anomalies of opposite sign between Antarctica and mid-latitudes (e.g., Thompson and Wallace, 2000), whereby positive atmospheric pressure anomalies at mid-latitudes together with negative anomalies at high latitudes indicate a +SAM and vice-versa for a SAM. Although SAM is defined as an annular mode, there is a strong non-annular regional component (Hall and Visbeck, 2002; van den Broeke and Lipzig, 2003; Lefebvre et al., 2004; Liu et al., 2004; Lefebvre and Goosse, 2005; Meredith et al., 2008). The non-annular component shows pressure anomalies roughly within the same area as described for ENSO above, with positive anomalies during SAM (similar to El Niño) and negative anomalies during +SAM (similar to La Niña).

Therefore, the variability in SLP anomalies averaged over 60–70°S and 65–100°W will have some association with the *regional* high-latitude atmospheric response to ENSO and/or SAM variability. Over 1979–2004 the month-to-month co-variability between ENSO and regional SLP (Fig. 7A), and SAM and regional SLP (Fig. 7B), was moderately strong (*R* ¼ +0.44, *R* ¼ 0.61, respectively). However, these relationships strengthened over 1992–2004, particularly during spring (Sep–Nov): *R* ¼ +0.53 and 0.73, respectively. Similarly, the month-to-month co-variability between ENSO and SAM, though weak over 1979–2004 (*R* ¼ 0.14; Fig. 7C), strengthened over 1992–2004, again particularly during spring (*R* ¼ 0.60) (see next section and also Fogt and Bromwich, 2006; Stammerjohn et al., 2008). In general, negative SLP anomalies to the west of the AP region (as can occur with La Niña and/or +SAM) indicate regional cyclonic (clockwise flowing) atmospheric circulation, with warm northerly winds over the wAP, thus generally *unfavorable* conditions for sea ice. In contrast, positive SLP anomalies to the west of the AP region (as can occur with El Niño and/or SAM) indicate regional

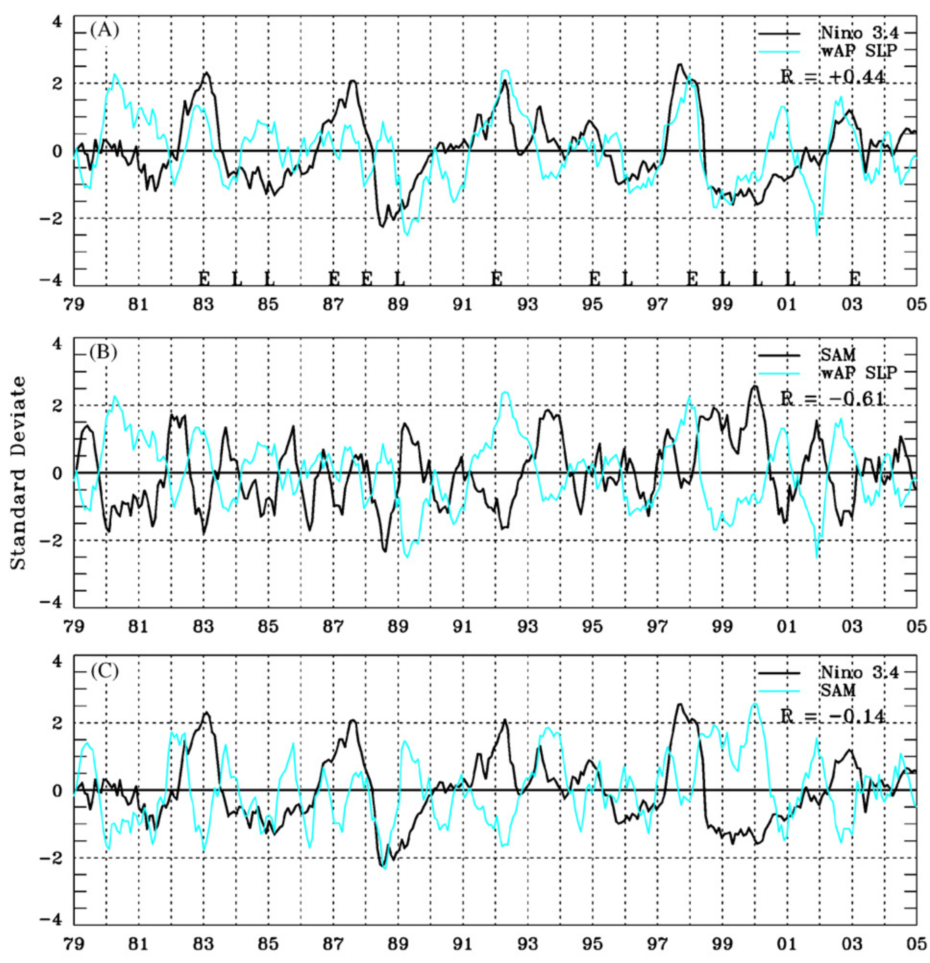

Fig. 7. 1979–2004 monthly time series of (A) Niño 3.4 index (black) and wAP SLP (blue), (B) SAM index (black) and wAP SLP (blue), and (C) Niño 3.4 (black) and SAM (blue) indices. The SAM index and wAP SLP were smoothed with a 7-month running mean. All time series are monthly anomalies normalized by the standard deviation. The wAP SLP data are from the region 60–70°S and 65–100°W.

anticyclonic (counterclockwise flowing) atmospheric circulation, with cold southerly winds over the wAP, thus *generally* favorable conditions for sea ice.

The location of the ice edge is sensitive to the strength and direction of the meridional wind, particularly in the wAP region (Stammerjohn et al., 2003; Turner et al., 2003; Harangozo, 2004, 2006; Harangozo and Connolley, 2006; Massom et al., 2006, 2008). The anomalies in the spring sea-ice retreat and subsequent autumn sea-ice advance are shown together with monthly wind anomalies for the period 1997–1998 to 2002–2003 (Fig. 8). This period coincides with strong transitions from El Niño (and slightly SAM) conditions in 1997–1998 to La Niña and +SAM conditions from the autumn of 1998 through to the spring of 2001 (though somewhat weakened in spring 2000 when SAM went negative), then back to El Niño and SAM conditions in 2002–2003. From the autumn of 1998 through to the spring–summer of 2001 the spring sea-ice retreat was often early, while the autumn advance was without a doubt late, consistent with the inferences from Fig. 7 that persistent northerly winds occurred in response to the sustained La Niña and +SAM conditions during this period.

The spring–summer of 2001–2002 is particularly noteworthy in that some of the strongest northerly winds in the wAP region were experienced from September to February. These winds facilitated an early sea-ice retreat offshore but a late sea-ice retreat inshore due to the compaction of sea ice against the Antarctic Peninsula that dynamically thickened sea ice up to 20 m in places (Massom et al., 2006). Thus, the ocean–atmosphere–ice–ecosystem responses on-to-offshore were varied and complex, all

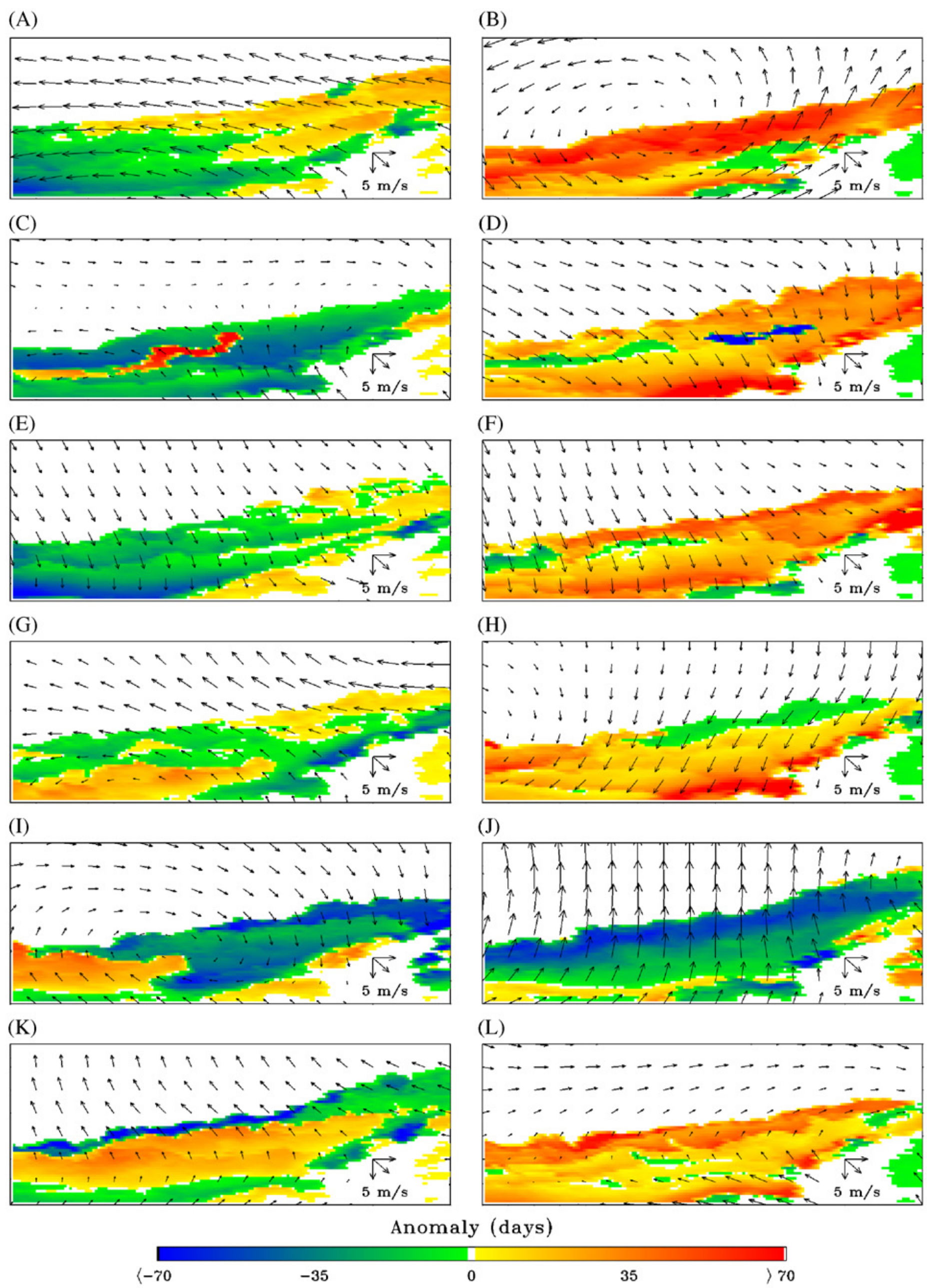

Fig. 8. (left column) Day of retreat anomalies with November wind anomalies overlaid; (right column) day of advance anomalies with May wind anomalies overlaid for (A) and (B) 1997–1998, (C) and (D) 1998–1999, (E) and (F) 1999–2000, (G) and (H) 2000–2001, (I) and (J) 2001–2002, and (K) and (L) 2002–2003. As for Figs. 4A and B, there is an anomalous trace caused by an iceberg in the 1998 sea-ice retreat (C, red squiggle) and 1999 sea ice advance (D, blue squiggle).

of which is described in detail by Massom et al. (2006). In addition, Martinson et al. (2008) show for 1998–2004 a positive trend in upper-ocean heat content within the PAL LTER area due to increases in the presence of UCDW on the shelf. However, January 2002 was a particularly large positive anomaly in ocean heat content, an outlier even with respect to the positive trend. The exceptionally strong northerly winds in the spring of 2001, as well as in the three preceding springs from 1998 to 2000, are implicated in causing the increased intrusions of UCDW on the shelf (and thus the increased upper-ocean heat content) in the late 1990s (Martinson et al., 2008). These wind-driven intrusions, co-occurring with wind-driven anomalies in sea-ice retreat and subsequent advance, are in turn associated with the high-latitude atmospheric response to La Niña and +SAM as described above.

In considering the potential for strong ocean–atmosphere–ice interactions and climate co-variability in the wAP region, the following key points are emphasized: (1) changes in ice season duration are caused mostly by changes in autumn sea-ice advance and to a lesser degree, the spring sea-ice retreat; (2) changes in the spring sea-ice retreat and subsequent autumn sea-ice advance, and by inference the frequency and/or intensity of UCDW intrusions on the shelf, are mostly in response to changes in the meridional winds (that can induce both a mechanical, wind-driven ice drift response and a thermodynamic response caused by warm/cold air advection); and (3) the presence of strong meridional winds in the wAP region are mostly in association with the high-latitude atmospheric response to ENSO and/or SAM variability.

3.4. *Sea ice trends and changes in ice-climate co-variability*

The 1979–2004 monthly sea-ice extent data for the PAL LTER region (Fig. 2) showed indications of trends towards earlier retreats and later advances. To view these changes spatially, climatologies were calculated for the earlier, pre-PAL LTER, period (1979–1991) and were subtracted from 1992 to 2004 (Fig. 9). The differences indicate tendencies towards (a) a later (positive difference) advance across the entire region; (b) an earlier (negative difference) retreat within the PAL LTER grid and south (versus a later retreat north of the grid); (c) fewer ice days (negative difference) across the entire region; and (d) higher persistence in the northern mid-grid vicinity, with near zero differences elsewhere. Within the PAL LTER grid area the magnitude of the difference is highest in the mid-shelf region (approximately between stations 50 and 100): mean day of advance occurred 20–30 days later, retreat 15–25 days earlier, and there were 30–40 fewer ice days during 1992–2004 versus 1979–1991. Over the full time series (1979–2004) trends were detected in most of the sea-ice characteristics (persistence excluded) and across most of the sub-regions (Table S2 in the Supplementary Online Material).

Ice-climate co-variability in the PAL LTER region, and changes therein, are summarized as follows (Fig. 10): (a) PAL LTER sea-ice extent negatively co-varies with Faraday/Vernadsky air temperature (1979–2004 monthly, *R* ¼ 0.79; annual, *R* ¼ 0.94); (b) 10-year running correlations show that co-variability decreased into the 1990s; (c) PAL LTER sea-ice extent positively co-varies with the ENSO Niño3.4 index (1979–2004 monthly, *R* ¼ 0.28; annual, *R* ¼ 0.47); and (d) 10-year running correlations show that co-variability between PAL LTER sea-ice extent and ENSO decreased into the 1990s and that co-variability between Faraday/Vernadsky air temperature and ENSO was generally low both before and after the 1980s (similar results to (b) and (d) are obtained when the SOI is used).

Concurrent with decreased climate co-variability in the 1990s is increased intra-seasonal variability in PAL LTER monthly sea-ice extent (Smith et al., 1998; Smith and Stammerjohn, 2001; Stammerjohn et al., 2008). The increase in intra-seasonal variability between the 1980s and 1990s (Fig. 2) is captured by the degree of persistence in monthly sea-ice extent anomalies, which decreased from 12 to 13 months in the 1980s to 2 months in the 1990s (based on autocorrelation analysis). Increased intra-seasonal variability is largely a result of increased variability in the timing of sea-ice advance and retreat in the 1990s.

In contrast to the analyses of monthly sea-ice extent and ENSO, correlations between the timing of sea-ice advance (as captured by PCA mode 1; Fig. 5A) versus seasonal averages of the ENSO index show increased correlations into the 1990s (Fig. 10E, lower solid curve). On the other hand, correlations between the timing of sea-ice retreat and ENSO (Fig. 10E, upper solid curve) are stronger in the 1980s, then show a slight decrease into the 1990s, but still remain higher than the correlations shown for monthly sea-ice extent (Fig. 10D). Given the increased intra-seasonal variability of sea ice in the wAP region, monthly sea-ice extent may not be the best variable for examining an ENSO relationship. The results presented here on sea-ice advance and retreat, in addition to results from Stammerjohn et al. (2008), seem to indicate that sea ice sensitivity to ENSO variability is better captured by restricting our focus to the periods (seasons) of sea-ice advance and retreat.

Trends in sea-ice retreat and subsequent advance are consistent with observed changes in ENSO and SAM variability in the 1990s: the high-latitude atmospheric response to ENSO intensified during austral spring–summer (e.g., Fogt and Bromwich, 2006) and SAM became more positive during summer–autumn (Marshall, 2003; Stammerjohn et al., 2008). The strengthening of the high-latitude atmospheric circulation in the 1990s during large ENSO events appears to be related to stronger and more *sustained* periods of co-variability between ENSO and SAM during spring-to-autumn. Concurrently, the positive trend in SAM (Thompson et al., 2000; Marshall, 2003) is implicated in asymmetrically strengthening the high-latitude response to La Niña over El Niño events. Stammerjohn et al. (2008) show that the episodic loss of sea ice during spring-to-autumn in the southern Bellingshausen region coincided with La Niña and/or +SAM events. The negative impacts resulting from these events resulted in remarkably large 26-year changes in the greater southern Bellingshausen Sea region: sea ice is retreating 317 10 days earlier and advancing 547 9 days later, resulting in a decrease of 857 20 annual sea-ice days over 1979–2004. The complete loss of summer sea ice in the southern Bellingshausen in 1998–1999 and 1999–2000 quite dramatically reflects the severe impacts resulting from co-occurring La Niña and +SAM events.

4. Discussion

4.1. *Ocean– atmosphere– ice interactions within the context of AP warming*

The strongest trends in surface air temperature in the AP region are during autumn and winter (King, 1994; King and Comiso, 2003; Vaughan et al., 2003), with July showing the strongest trend: a 6.5 °C increase over 1950–2005 (http://www.antarctica.ac.uk/met/gjma/temps.html). Concurrently, the strongest trend in sea ice in the greater wAP region is a later sea-ice advance in autumn/early winter. Delayed sea-ice advance in the wAP region has been associated with increased northerly winds (Fig. 8). The increased northerly winds infer that the ice-edge advance is hampered by the constant advection of sea ice

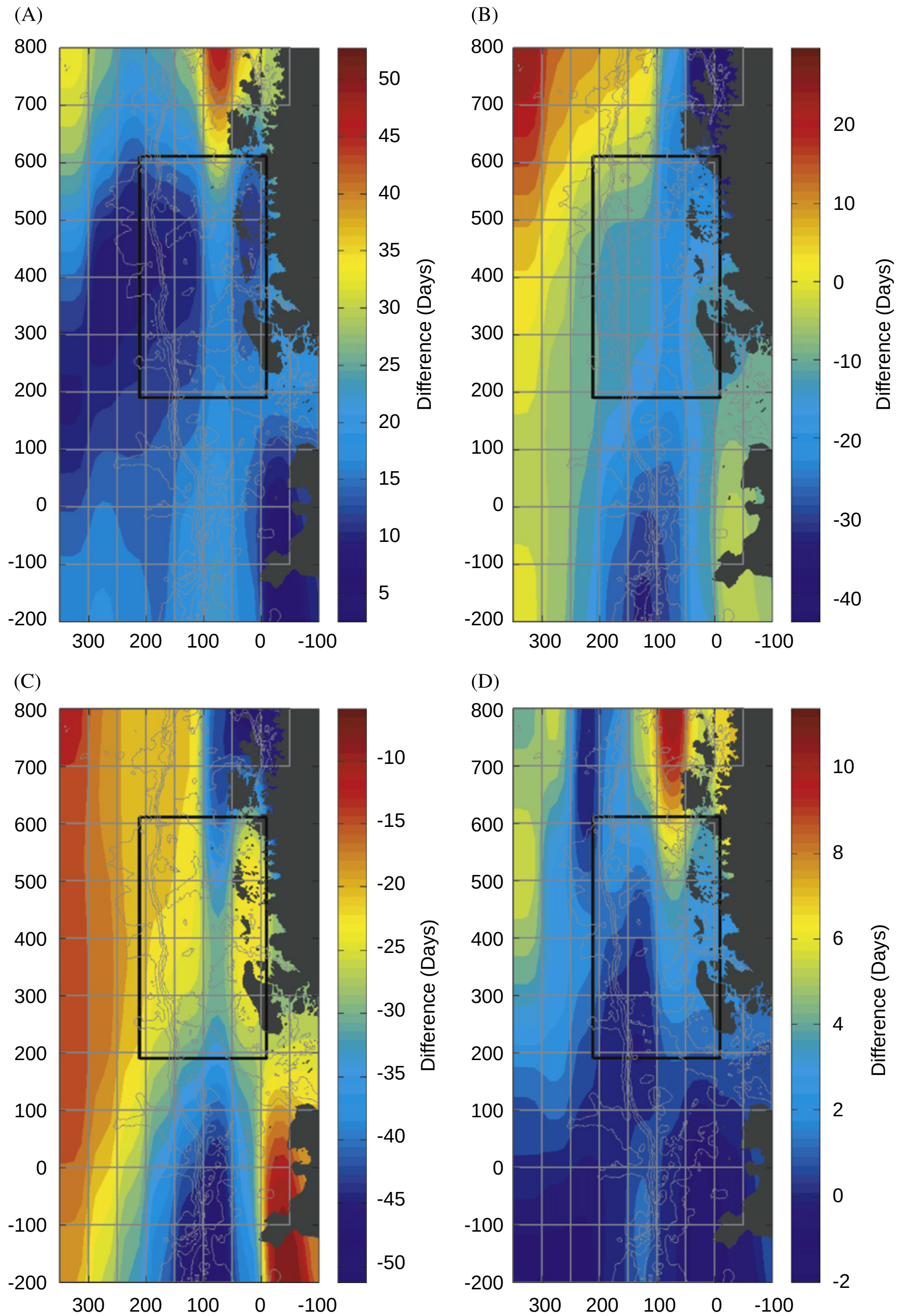

Fig. 9. Spatial maps of the difference between the 1992 and 2004 climatology minus the 1979–1991 climatology for (A) day of advance, (B) day of retreat, (C) ice days, and (D) ice persistence (%). In gray are rectangular grid cells (50 100 km) and bathymetry contoured at 500, 1000, 2000 and 3000 m depth levels. Where there are no grid cells (e.g., lower right corner, around land), values are spatially interpolated.

southeastward toward the coast. Without an insulating sea-ice cover, the ocean heat flux to the atmosphere dramatically increases. Thus, the trend towards a later sea-ice advance is (1) an indicator of increased northerly winds, which advect warm air into the region from lower latitudes, and (2) facilitates increased ocean heat flux, which vents ocean heat to the overlying atmosphere. The increase in both warm air advection and open-ocean heat flux would contribute to, and/or amplify, warming in the AP region in autumn/early winter, as suggested by others (Vaughan et al., 2003; Meredith and King, 2005; Harangozo, 2006). In particular, the ice–ocean response serves as a strong positive feedback on what is believed to be a regional expression of global warming.

In addition, there is the potential for inter-seasonal feedbacks well into winter. The trend towards a later sea-ice advance (and somewhat earlier sea-ice retreat) results in decreased winter sea-ice days. A shorter sea-ice season implies less time for sea ice to thicken (both thermodynamically and mechanically). The strong co-variability between the summer mixed layer freshwater content and the previous winter's ice days (Fig. 6) also infers that the number of ice days serves as a proxy for ice volume. Additionally, a trend towards decreased sea-ice concentration (e.g. Liu et al., 2004) and a seasonally more variable sea-ice cover (Fig. 2B) imply thinner sea ice and/or increased lead fraction. Decreased winter sea-ice duration, concentration, thickness and/or increased lead fraction are changes that would continue to drive

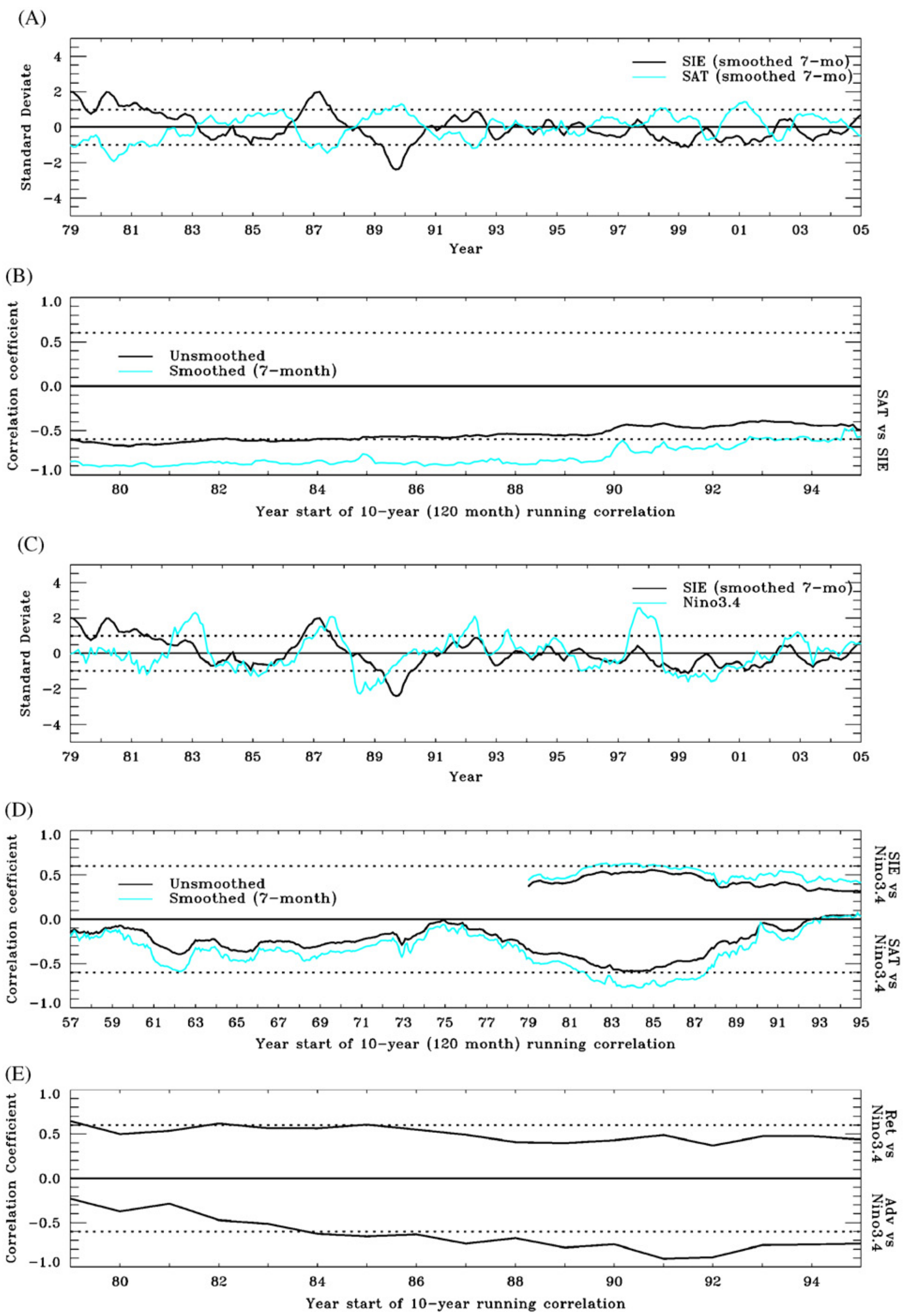

Fig. 10. (A) 1979–2004 time series of monthly anomalies (normalized by the standard deviation) of PAL LTER sea ice extent (SIE) and Faraday/Vernadsky surface air temperature (SAT), (B) 10-year running correlations between SIE and SAT, (C) 1979–2004 time series of normalized anomalies of SIE and the Niño 3.4 ENSO index, (D) 10-year running correlations between SIE and Niño 3.4 index, and between SAT and Niño 3.4 index, and (E) 10-year running correlations between the first principal component (PC1) of sea-ice advance (adv) and Niño 3.4, and between PC1 of sea-ice retreat (ret) and Niño 3.4. In (A) and (C) the SIE time series were smoothed with a 7-month running average, and in (B) and (D) SIE and SAT were first smoothed with a 7-month running average (blue lines) before computing running correlations.

an increased ocean heat flux to the overlying atmosphere throughout winter (Martinson et al., 2008).

Examples of ice-atmosphere co-variability in the PAL LTER region (Fig. 11) lend further support to the working hypothesis described above. Beginning in spring (Sep–Nov), winds strongly co-vary with the spring–summer sea-ice retreat in the PAL LTER coastal region (*R* ¼ +0.87) such that strong winds are associated with a late coastal sea-ice retreat, and vice-versa for weak winds (Fig. 11A). The implication is that the strong spring winds dynamically thicken the sea ice via compaction against the coast (as described by Massom et al., 2006), and the dynamically thickened sea ice then takes longer to melt (retreat). In turn, the variability in the spring–summer coastal sea-ice retreat strongly co-varies with coastal summer (Dec–Feb) air temperature (*R* ¼ 0.72) such that a late spring–summer coastal sea-ice retreat induced by strong spring winds is associated with cool summer coastal air temperature, and vice-versa for an early coastal sea-ice retreat (Fig. 11B). In autumn (Mar–May) winds strongly co-vary with sea-ice advance over the shelf (*R* ¼ +0.61) such that high winds are associated with a late autumn sea-ice advance, and vice-versa for low winds (Fig. 11C). In turn, the autumn sea-ice advance over the shelf strongly co-varies with

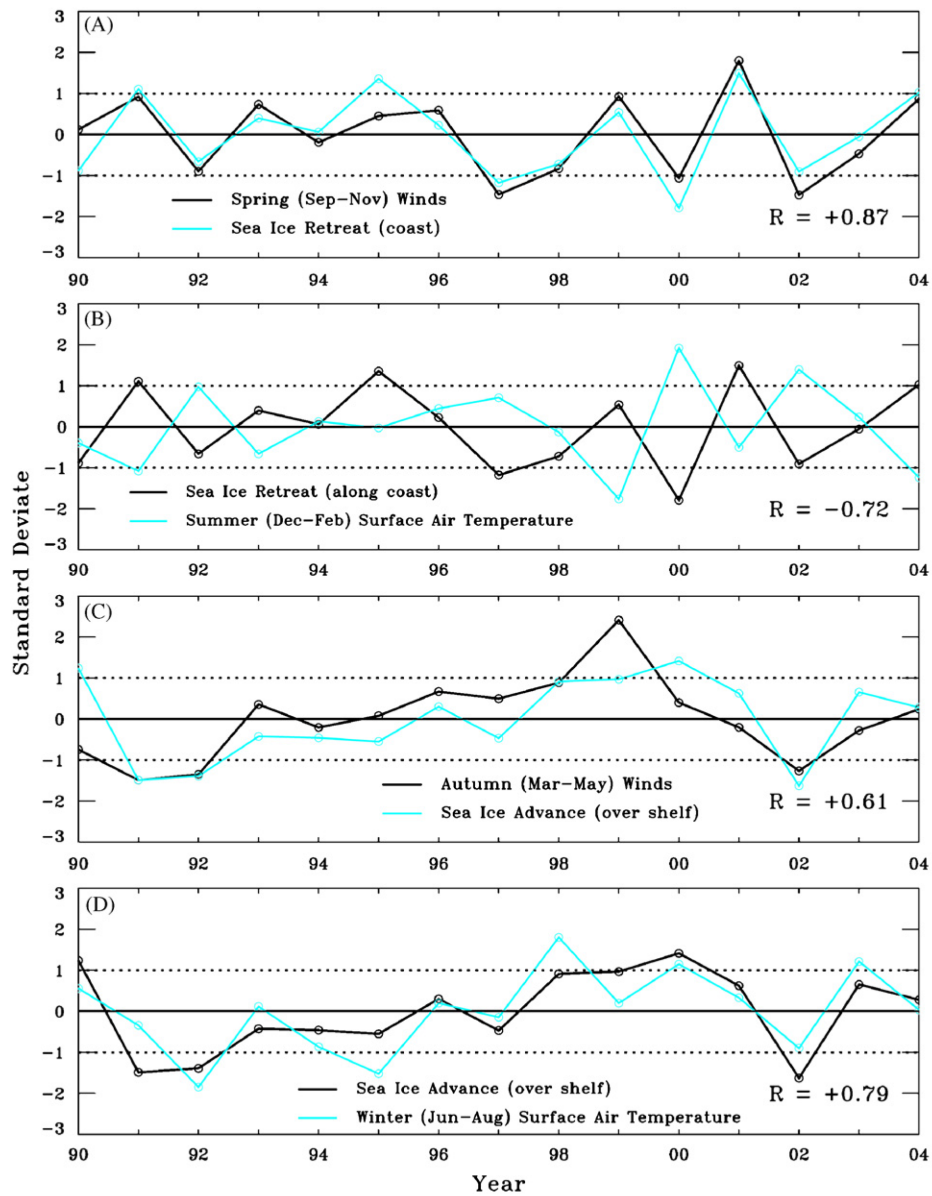

Fig. 11. 1990–2004 time series of normalized anomalies of (A) spring (Sep–Nov) winds averaged for the central wAP area and the spring sea-ice retreat in the central coast region (*R* ¼ +0.87); (B) the spring sea-ice retreat in the central coast region and summer (Dec–Feb) surface air temperature at Faraday/Vernadsky (*R* ¼ 0.72); (C) Autumn (Mar–May) winds averaged for the northern wAP area and the autumn sea-ice advance over the northern shelf (*R* ¼ +0.61); and (D) the autumn sea-ice advance and winter (Jun–Aug) surface air temperature at Faraday/Vernadsky (*R* ¼ +0.79).

winter (Jun–Aug) coastal air temperature (*R* ¼ +0.79) such that a late autumn sea-ice advance induced by strong northerly winds is associated with warm winter air temperature (Fig. 11D). The correlation between sea-ice days and winter air temperature is not quite as strong (*R* ¼ 0.50) as that shown for sea-ice advance and winter air temperature (Fig. 11D), but may be suggestive of the continued influence of ice–ocean interactions on air temperature throughout the winter (e.g., less ice days, more ocean heat flux to the overlying atmosphere).

4.2. Ice– ecosystem interactions and change

The central hypothesis of the PAL LTER states that the seasonal and interannual variability of sea ice affects all levels of the Antarctic marine ecosystem, from the timing and magnitude of seasonal primary production to the breeding success and survival of apex predators. In addressing the former (seasonal primary production), the timing of the spring sea-ice retreat in the wAP region has some association with when and where the spring-summer phytoplankton blooms occur (Garibotti et al., 2005; Smith et al., 2008), but these associations are not always consistent across the wAP region, particularly off-to-onshore. For example, sea-ice retreat was late offshore of the shelf break during Oct–Nov in 1997 and 2002 (i.e. was still over the SACCF region in November), and consequently the offshore spring bloom did not occur. Subsequent to the late retreat offshore, the retreat over the inshore shelf area was relatively early, and chl-*a* biomass concentrations were low in Jan–Feb of 1998 and 2003 (Smith et al., 2008), presumably due to a lack of a well-developed ice-edge bloom. Therefore, a late retreat offshore of the shelf break region and an early retreat over the shelf were associated with low pigment biomass in both of these locations.

In contrast, the retreat in 1995 and 2001 was early offshore of the shelf break and late inshore, and subsequently the chl-*a* concentration within the PAL LTER in Jan 1996 and 2002 were two of the highest grid averages measured during 1994–2004 (Vernet et al., 2008). The pigment biomass concentrations also were high offshore of the shelf break in 2001, and we presume in 1995 as well, but SeaWiFs data only became available starting in 1997. In further contrast, the lowest chl-*a* concentrations detected within the PAL LTER were in Jan 1999 and the previous spring retreat was early across the *entire* wAP region. But, despite the low concentrations detected within the PAL LTER region in Jan 1999, the SeaWiFs imagery shows a well-developed bloom offshore of the shelf break that started as early as October, presumably in response to the earlier sea-ice retreat for this location. Therefore, the associations between anomalies in the timing of the spring sea-ice retreat and phytoplankton biomass concentration are spatially and seasonally mixed. In general, however, these various studies indicate that an early sea-ice retreat offshore of the shelf break favors a spring bloom in this location, whereas a later sea-ice retreat over the shelf and along the coast favors a summer bloom in that location. Massom et al. (2006) give further examples of complex ice–ecosystem interactions that resulted from anomalous ice–atmosphere interactions in 2001–2002 that in turn resulted in strong off-to-onshore sea-ice retreat anomalies that had both positive and negative impacts on the marine ecosystem.

Though there appear to be clear associations between the timing of sea-ice retreat and phytoplankton biomass, other associations with higher trophic levels (e.g., zooplankton, seabirds) are more complex. There are indications that fewer sea-ice days, when coupled with an early sea-ice retreat, may be unfavorable for krill reproduction (but favorable for other zooplankton species such as Salps) (Ross et al., 2008). Fewer sea-ice days, if indicative of sea-ice thickness, also may be unfavorable for juvenile krill, given that a thicker, rafted sea-ice cover provides a better underwater refuge (Quetin et al., 1996; Frazer et al., 1997; Ross et al., 2004; Massom et al., 2006).

Consequently, any decreases in krill recruitment or availability will adversely affect predator populations (e.g., Adélie penguins) via changes in predator foraging and breeding performance (Fraser and Hofmann, 2003). Increased occurrences of earlier sea-ice retreat are associated with increased storminess and precipitation, conditions unfavorable for Adélie penguin egg laying (Fraser and Patterson, 1997; Patterson et al., 2003; Massom et al., 2006). Deep snow at penguin nesting colonies has been associated with increased egg mortality caused by the formation of snowmelt pools at the nest. Other ice-mediated factors like foraging trip durations during spring breeding, food availability to fledging chicks in summer, ice-edge foraging in winter, affect Adélie penguin recruitment and mortality. The observation that Adélie penguins are rapidly declining in the Palmer Basin area (Ducklow et al., 2007) is strong supporting evidence that ice-ecosystem changes have quite drastically occurred in the wAP region in response to the rapid regional climate change (Ross et al., 1996; Smith et al., 1999; Domack et al., 2003; Smetacek and Nicol, 2005, and other references in this special DSR-II issue).

5. Summary

The spatial and temporal (1992–2004) variability of sea ice has been described for the PAL LTER and greater wAP region using four sea-ice characteristics that capture key components of the annual cycle of sea ice: (1) day of advance, (2) day of retreat, (3) number of sea-ice days and (4) sea-ice persistence. We also examined the co-variability between upper-ocean summer mixed layer properties and sea ice the previous winter. Ice-atmosphere anomalies in association with ENSO and SAM variability were described, and changes in climate co-variability and trends were assessed. The following is a summary of key findings:

(1) The strongest geographical distinction across the PAL LTER grid is the longer sea-ice season in the coastal regions (6.8–7.9 months) versus the shorter sea-ice season over the shelf (4.1–5.3 months), these on-to-offshore differences increasing south-to-north. In general, coastal environments are more complex. For example, the northern coastal region (Palmer Basin vicinity) is characterized as having a long ice season, but nearly half of this season is characterized by loose, open pack-ice conditions (i.e., concentrations less than 50%), consistent with more frequent opening and closing of the pack ice throughout the winter and relatively high year-to-year variability. In contrast, the southern coastal region (Marguerite Bay vicinity) has a long sea-ice season characterized by heavy sea-ice conditions (i.e. concentrations greater than 50%), fewer opening and closing events throughout the season and relatively low year-to-year variability.

(2) The temporal and spatial variability of sea-ice advance in the wAP region is distinctly different from that of sea-ice retreat, thus differently affecting the duration of the sea-ice season. Due to the free (unconstrained) expansion of sea ice during advance, the temporal variability of sea-ice advance is more spatially coherent across the PAL LTER grid and co-varies more strongly with ice season duration (than does retreat). Overall, sea-ice advance appears to be more sensitive to climate variability given that it can quickly and coherently respond to changes in atmospheric conditions. In contrast, sea-ice retreat is more variable both in space and time, and the movement of sea ice during retreat is heavily constrained by increasing thickness to the south and the geographic barrier of the peninsula.

(3) The freshwater content of the summer surface mixed layer within the PAL LTER grid strongly co-varies with the number of ice days the previous winter (e.g., high freshwater content co-occurs with high number of ice days) for all but the northern coast region (where glacial meltwater input appears to be a significant contributor of freshwater) and to a lesser degree the southern shelf-break region (where UCDW may be influencing surface mixed-layer freshwater content). In contrast to freshwater content, the heat content of the summer surface mixed layer primarily reflects surface air temperature variability but also coincides with the timing of the spring sea-ice retreat (e.g., earlier retreat, greater heat content) except during outlier years when spring–summer air temperature was cool (and heat content low) but sea-ice retreat was early (and vice-versa) as often happened in the latter half of the 1979–2004 record.

(4) Anomalies in sea-ice advance and total ice days show a grid wide shift from 1992–1997 to 1998–2001. The former period was characterized by earlier sea-ice advance and higher numbers of ice days, while the latter period was characterized by later sea-ice advance and lower numbers of ice days. Persistent northerly winds, particularly during the autumns of 1998–2001, appeared to contribute to the delayed sea-ice advance over this period. In turn, these anomalous atmospheric circulation anomalies were associated with a period of sustained La Niña and +SAM conditions. The spring–summer 2001–2002 was particularly noteworthy given the severity and persistence of the northerly winds in the PAL LTER region from September to February. As detailed by Massom et al. (2006) the ocean–atmosphere–ice-ecosystem responses to this extreme atmospheric forcing event were varied and complex.

(5) Trend analyses of PAL LTER sea-ice characteristics indicated that over the shelf the mean day of advance was occurring 20–30 days later, the retreat 15–25 days earlier, and there were 30–40 fewer ice days in 1992–2004 relative to 1979–1991. Changes in ice season duration are caused mostly by changes in autumn sea-ice advance and to a lesser degree the spring sea-ice retreat. The largest anomalies towards a somewhat earlier retreat and a much later advance co-occur with strong northerly winds during La Niña and/or +SAM.

(6) Ocean–atmosphere–ice interactions and trends are consistent with the overall rapid regional warming of the Antarctic Peninsula region: (a) the trends towards a delayed autumn advance is an indication of increased northerly winds (which advect warm air into the region from lower latitudes) and facilitates increased ocean heat flux (which vents ocean heat to the overlying atmosphere); (b) the trend towards a shorter sea-ice season is concurrent with a decrease in sea-ice concentration and an increase in intra-seasonal variability, changes that infer relatively thinner sea ice and/or increased lead fraction and therefore increased ocean heat fluxes to the atmosphere throughout winter; and (c) together, these seasonal sea ice-mediated changes (i.e., increased warm air advection and increased ocean heat flux) would contribute to, and/or amplify, warming in the AP region in autumn/early winter as suggested by others (Vaughan et al., 2003; Meredith and King, 2005; Harangozo, 2006). The ice–ocean response in particular serves as a strong positive feedback on what is believed to be a regional expression of global warming.

Acknowledgements

This work was largely supported by a NASA Fellowship Grant NGT5-30391 and leveraged by National Ocean and Atmosphere Administration Grant/Cooperative Agreement NA17RJ1231 (SES), as well as by Palmer LTER NSF/OPP 0217282 (SES, DGM, RCS, RI). The paper was finalized with support from the NOAA Climate and Global Change Postdoctoral Fellowship Program administered by the University Corporation for Atmospheric Research and conducted at the NASA Goddard Institute of Space Studies (SES). The 1979–2004 SMMR-SSM/I sea ice concentration data were from the EOS Distributed Active Archive Center (DAAC) at the National Snow and Ice Data Center, University of Colorado in Boulder, Colorado (http://nsidc.org). The sea-level pressure and 10-m wind data were from the National Center for Environmental Prediction/National Center for Atmospheric Research (NCEP/NCAR) Reanalysis Project. Gareth Marshall provided the SAM index data (http://www.nercbas.ac.uk/icd/gjma/sam.html), and the International Research Institute for Climate Prediction the Niño3.4 index data (http://iridl.ldeo.columbia.edu/). This paper greatly benefited from discussions with Maria Vernet, Robin Ross, Langdon Quetin, Hugh Ducklow, Bill Fraser, Xiaojun Yuan and David Rind, as well as from the generous efforts of two anonymous reviewers. This is Palmer LTER contribution No. 0296, and LDEO Contribution No. 7057.

Appendix A. Supporting Information

Supplementary data associated with this article can be found in the online version at doi:10.1016/j.dsr2.2008.04.026.

References

Cane, M.A., Zebiak, S.E., Dolan, S.C., 1986. Experimental forecasts of El Nino. Nature 322, 827–832.

Comiso, J., 2003. Sea ice concentrations derived from the Bootstrap algorithm. In: Maslanik, J., Stroeve, J. (Eds.), DMSP SSM/I Daily Polar Gridded Sea Ice Concentrations. Digital Media, National Snow and Ice Data Center, Boulder, CO.

Comiso, J.C., 1995. Sea-ice geophysical parameters from SMMR and SSM/I data. In: Ikeda, M., Dobson, F. (Eds.), Oceanographic Applications of Remote Sensing. CRC Press, London, UK, pp. 321–338.

Comiso, J.C., Cavalieri, D., Parkinson, C., Gloersen, P., 1997. Passive microwave algorithms for sea ice concentration—a comparison of two techniques. Remote Sensing of the Environment 60 (3), 357–384.

Dierssen, H.M., Smith, R.C., Vernet, M., 2002. Glacial meltwater dynamics in coastal waters west of the Antarctic Peninsula. Proceedings of the National Academy of Sciences 99, 1790–1795.

Domack, E., Leventer, A., Burnett, A., Bindschadler, R., Convey, P., Kirby, M., 2003. Antarctic Peninsula Climate Variability: Historical and Paleoenvironmental Perspectives, Antarctic Research Series 79. American Geophysical Union, Washington, DC, p. 272.

Ducklow, H.W., Baker, K., Martinson, D.G., Quetin, L.B., Ross, R.M., Smith, R.C., Stammerjohn, S.E., Vernet, M., Fraser, W., 2007. Marine pelagic ecosystems: the West Antarctic Peninsula. Philosophical Transactions of the Royal Society B 362, 67–94.

Fogt, R.L., Bromwich, D.H., 2006. Decadal variability of the ENSO teleconnection to the high latitude South Pacific governed by coupling with the Southern Annular Mode. Journal of Climate 19, 979–997.

Fraser, W.R., Hofmann, E.E., 2003. A predator's perspective on causal links between climate change, physical forcing and ecosystem response. Marine Ecology Progress Series 265, 1–15.

Fraser, W.R., Patterson, D.L., 1997. Human disturbance and long-term changes in Adélie penguin populations: a natural experiment at Palmer Station, Antarctic Peninsula. In: Battaglia, B., Valencia, J., Walton, D.W.H. (Eds.), Antarctic Communities: Species, Structure and Survival. Cambridge University Press, New York, NY, pp. 445–452.

Frazer, T.K., Quetin, L.B., Ross, R.M., 1997. Abundance and distribution of larval krill, *Euphausia superba*, associated with annual sea ice in winter. In: Battaglia, B., Valencia, J., Walton, D.W.H. (Eds.), Antarctic Communities: Species, Structure and Survival. Cambridge University Press, New York, NY, pp. 107–111.

Garibotti, I.A., Vernet, M., Ferrario, M.E., 2005. Annually recurrent phytoplanktonic assemblages during summer in the seasonal ice zone west of the Antarctic Peninsula (Southern Ocean). Deep Sea Research I 52, 1823–1841.

Hall, A., Visbeck, M., 2002. Synchronous variability in the Southern Hemisphere atmosphere, sea ice and ocean resulting from the Annular Mode. Journal of Climate 15, 3043–3057.

Harangozo, S.A., 2000. A search for ENSO teleconnections in the west Antarctic Peninsula climate in austral winter. International Journal of Climatology 20 (6), 663–679.

Harangozo, S.A., 2004. The impact of winter ice retreat on Antarctic winter sea-ice extent and links to the atmospheric meridional circulation. International Journal of Climatology 24, 1023–1044.

Harangozo, S.A., 2006. Atmospheric circulation impacts on winter maximum sea ice extent in the west Antarctic Peninsula region (1979–2001). Geophysical Research Letters 33 [doi:10.1029/2005GL024978].

Harangozo, S.A., Connolley, W.M., 2006. The role of the atmospheric circulation in the record minimum extent of open water in the Ross Sea in the 2003 austral summer. Atmosphere-Ocean 44 (1), 83–97.

Holland, M.M., Bitz, C.M., Hunke, E., 2005. Mechanisms forcing an Antarctic Dipole in simulated sea ice and surface ocean conditions. Journal of Climate 18, 2052–2066.

Kalnay, E., Kanamitsu, M., Kistler, R., Collins, W., Deaven, D., Gandin, L., Iredell, M., Saha, S., White, G., Woollen, J., Zhu, Y., Chelliah, M., Ebisuzaki, W., Higgins, W., Janowiak, J., Mo, K.C., Ropelewski, C., Wang, J., Leetmaa, A., Reynolds, R., Jenne, R., Joseph, D., 1996. The NCEP/NCAR 40-year reanalysis project. Bulletin of American Meteorological Society 77, 437–471.

King, J.C., 1994. Recent climate variability in the vicinity of the Antarctic Peninsula. International Journal of Climatology 14 (4), 357–369.

King, J.C., Comiso, J.C., 2003. The spatial coherence of interannual temperature variations in the Antarctic Peninsula. Geophysical Research Letters 30 (2) [doi:10.1029/2002GL015580].

Kwok, R., Comiso, J.C., 2002. Southern Ocean climate and sea ice anomalies associated with the Southern Oscillation. Journal of Climate 15, 487–501.

Lachlan-Cope, T., Connolley, W., 2006. Teleconnections between the tropical Pacific and the Amundsen–Bellingshausen Sea: role of the El Nino/Southern Oscillation. Journal of Geophysical Research 111 [doi:10.1029/2005JD006386].

Lefebvre, W., Goosse, H., 2005. Influence of the Southern Annular Mode on the sea ice–ocean system: the role of the thermal and mechanical forcing. Ocean Sciences 1, 145–157.

Lefebvre, W., Goosse, H., 2008. An analysis of the atmospheric processes driving the large-scale winter sea-ice variability in the Southern Ocean. Journal of Geophysical Research 113 (C02004) [doi:10.1029/2006JC004032].

Lefebvre, W., Goosse, H., Timmermann, R., Fichefet, T., 2004. Influence of the Southern Annular Mode on the sea ice–ocean system. Journal of Geophysical Research 109 [doi:10.1029/2005JD006386].

Liu, J., Curry, J.A., Martinson, D.G., 2004. Interpretation of recent Antarctic sea ice variability. Geophysical Research Letters 31, L02205 [doi:10.1029/2003GL018732].

Marshall, G.J., 2003. Trends in the Southern Annular Mode from observations and reanalyses. Journal of Climate 16, 4134–4143.

Marshall, G.J., Orr, A., van Lipzig, N.P.M., King, J.C., 2006. The impact of a changing Southern hemisphere annular mode on Antarctic Peninsula summer temperature. Journal of Climate 19, 5388–5404.
Martinson, D.G., 1990. Evolution of the Southern Ocean winter mixed layer and sea ice: open ocean deepwater formation and ventilation. Journal of Geophysical Research 95, 11641–11654.
Martinson, D.G., Iannuzzi, R.A., 1998. Antarctic ocean-ice interaction: implications from ocean bulk property distributions in the Weddell gyre. In: Jeffries, M.O. (Ed.), Antarctic Sea Ice: Physical Processes, Interactions and Variability, Antarctic Research Series 74. American Geophysical Union, Washington, DC, pp. 243–271.
Martinson, D.G., Stammerjohn, S.E., Iannuzzi, R.A., Smith, R.C., Vernet, M., 2008. Western Antarctic Peninsula physical oceanography and spatio-temporal variability, this issue [doi:10.1016/j.dsr2.2008.04.038].
Massom, R.A., Stammerjohn, S.E., Smith, R.C., Pook, M.J., Iannuzzi, R., Adams, N., Martinson, D., Vernet, M., Fraser, W.R., Quetin, L.B., Ross, R.M., Massom, Y., Krouse, H.R., 2006. Extreme anomalous atmospheric circulation in the west Antarctic Peninsula region in austral spring and summer 2001/2, and its profound impact on sea ice and biota. Journal of Climate 19, 3544–3571.
Massom, R.A., Stammerjohn, S.E., Lefebvre, W., Harangozo, S.A., Adams, N., Scambos, T.A., Pook, M.J., Fowler, C., 2008. West Antarctic Peninsula sea ice in 2005: Extreme ice compaction and ice edge retreat due to strong anomaly with respect to climate. Journal of Geophysical Research 113 (C02S20) [doi:10.1029/2007JC004239].
Meredith, M.P., Hogg, A.M., 2006. Circumpolar response of Southern Ocean eddy activity to changes in the Southern Annular Mode. Geophysical Research Letters 33 (16) [doi:10.1029/2006GL026499].
Meredith, M.P., King, J.C., 2005. Rapid climate change in the ocean west of the Antarctic Peninsula during the second half of the 20th century. Geophysical Research Letters 32 [doi:10.1029/2005GL024042].
Meredith, M.P., Renfrew, I.A., Clarke, A., King, J.C., Brandon, M.A., 2004a. Impact of the 1997/98 ENSO on the upper waters of Marguerite Bay, western Antarctic Peninsula. Journal of Geophysical Research 109 [doi:10.1029/2003JC001784].
Meredith, M.P., Woodworth, P.L., Hughes, C.W., Stepanov, V., 2004b. Changes in the ocean transport through Drake Passage during the 1980s and 1990s, forced by changes in the Southern Annular Mode. Geophysical Research Letters 31 [doi:10.1029/2004GL021169].
Meredith, M.P., Murphy, E.J., Hawker, E.J., King, J.C., Wallace, M.I., 2008. On the interannual variability of ocean temperatures around South Georgia, Southern Ocean: forcing by El Nino/Southern Oscillation and the Southern Annular Mode, Deep-Sea Research II, this issue [doi:10.1016/j.dsr2.2008.05.020].
Parkinson, C.L., 2002. Trends in the length of the Southern Ocean Sea Ice Season, 1979–1999. Annals of Glaciology 34, 435–440.
Parkinson, C.L., 2004. Southern Ocean sea ice and its wider linkages: insights revealed from models and observations. Antarctic Science 16 (4), 387–400.
Patterson, D.L., Easter-Pilcher, A., Fraser, W.R., 2003. The effects of human activity and environmental variability on long-term changes in Adelie penguin populations at Palmer Station, Antactica. In: Huiskes, A.H.L., Gieskes, W.W.C., Rozema, J., Schorno, R.M.L., van der Vies, S.M., Wolff, W.J. (Eds.), Antarctic Biology in a Global Context, Scientific Committee for Antarctic Research (SCAR), Eighth Biological Symposium, The Netherlands, pp. 301–307.
Quetin, L.B., Ross, R.M., Frazer, T.K., Haberman, K.L., 1996. Factors affecting distribution and abundance of zooplankton, with an emphasis on Antarctic krill, *Euphausia superba*. In: Ross, R.M., Hofmann, E.E., Quetin, L.B. (Eds.), Foundations for Ecological Research west of the Antarctic Peninsula, Antarctic Research Series 70. American Geophysical Union, Washington, DC, pp. 357–371.
Ross, R.M., Hofmann, E.E., Quetin, L.B., 1996. Foundations for Ecological Research West of the Antarctic Peninsula, Antarctic Research Series 70. American Geophysical Union, Washington, DC, p. 448.
Ross, R.M., Quetin, L.B., Newberger, T.A., Oakes, S.A., 2004. Growth and behavior of larval krill (*Euphausia superba*) under the ice in late winter 2001 west of the Antarctic Peninsula. Deep-Sea Research II 51, 2169–2184.
Ross, R.M., Quetin, L.B., Martinson, D.G., Iannuzzi, R.A., Stammerjohn, S.E., Smith, R.C., 2008. Patterns of distribution of five dominant zooplankton species in the epipelagic zone west of the Antarctic Peninsula, 1993–2004, Deep-Sea Research II, this issue [doi:10.1016/j.dsr2.2008.04.037].
Sen Gupta, A., England, M.H., 2006. Coupled ocean–atmosphere–ice response to variations in the Southern Annular Mode. Journal of Climate 19, 4457–4486.
Simmonds, I., Jacka, T.H., 1995. Relationships between the interannual variability of Antarctic sea ice and the Southern Oscillation. Journal of Climate 8, 637–647.
Smetacek, V., Nicol, S., 2005. Polar ocean ecosystems in a changing world. Nature 437, 362–368.
Smith, R.C., Stammerjohn, S.E., 2001. Variations of surface air temperature and sea ice extent in the western Antarctic Peninsula (WAP) region. Annals of Glaciology 33, 493–500.
Smith, R.C., Baker, K.S., Fraser, W.R., Hofmann, E.E., Karl, D.M., Klinck, J.M., Quetin, L.B., Prezelin, B.B., Ross, R.M., Trivelpiece, W.Z., Vernet, M., 1995. The Palmer LTER: a long-term ecological research program at Palmer Station, Antarctica. Oceanography 8 (3), 77–86.
Smith, R.C., Baker, K.S., Stammerjohn, S.E., 1998. Exploring sea ice indexes for polar ecosystem studies. BioScience 48 (2), 83–93.
Smith, R.C., Ainley, D., Baker, K., Domack, E., Emslie, S., Fraser, W., Kennett, J., Leventer, A., Mosley-Thompson, E., Stammerjohn, S., Vernet, M., 1999. Marine ecosystem sensitivity to climate change. BioScience 49 (5), 393–404.
Smith, R.C., Martinson, D.G., Stammerjohn, S.E., Iannuzzi, R.A., Ireson, K., 2008. Bellingshausen and western Antarctic Peninsula region: Pigment biomass and sea-ice spatial/temporal distributions and interannual variability, Deep-Sea Research II, this issue [doi:10.1016/j.dsr2.2008.04.027].
Stammerjohn, S.E., Drinkwater, M.R., Smith, R.C., Liu, X., 2003. Ice-atmosphere interactions during sea-ice advance and retreat in the western Antarctic Peninsula region. Journal of Geophysical Research 108 (C10) [doi:10.1029/2002JC001543].
Stammerjohn, S.E., Martinson, D.G., Smith, R.C., Yuan, X., Rind, D., 2008. Trends in Antarctic annual sea ice retreat and advance and their relation to El Nino-Southern Oscillation and Southern Annular Mode variability. Journal of Geophysical Research 113 (C03S90) [doi:10.1029/2007JC004269].
Stammerjohn, S.E., Smith, R.C., 1996. Spatial and temporal variability of western Antarctic Peninsula sea ice coverage. In: Ross, R.M., Hofmann, E.E., Quetin, L.B. (Eds.), Foundations for Ecological Research West of the Antarctic Peninsula, Antarctic Research Series 70. American Geophysical Union, Washington, DC, pp. 81–104.
Stammerjohn, S.E., Smith, R.C., 1997. Opposing Southern Ocean climate patterns as revealed by trends in regional sea ice coverage. Climatic Change 37 (4), 617–639.
Steele, J.H., 1991. Can ecological theory cross the land-sea boundary. Journal of Theoretical Biology 153, 425–436.
Thompson, D.W.J., Solomon, S., 2002. Interpretation of recent Southern Hemisphere climate change. Science 296, 895–899.
Thompson, D.W.J., Wallace, J.M., 2000. Annual modes in the extratropical circulation. Part I: month-to-month variability. Journal of Climate 13, 1000–1016.
Thompson, D.W.J., Wallace, J.M., Hegerl, G.C., 2000. Annular modes in the extratropical circulation. Part II: trends. Journal of Climate 13, 1018–1036.
Tréguer, P., Jacques, G., 1992. Dynamics of nutrient and phytoplankton and cycles of carbon, nitrogen and silicon in the Southern Ocean: a review. Polar Biology 12, 149–162.
Turner, J., 2004. Review: the El Niño-Southern oscillation and Antarctica. International Journal of Climate 24, 1–31.
Turner, J., Harangozo, S.A., King, J.C., Connolley, W.M., Lachlan-Cope, T.A., Marshall, G.J., 2003. An exceptional winter sea-ice retreat/advance in the Bellingshausen Sea, Antarctica. Atmosphere-Ocean 41 (2), 171–185.
van den Broeke, M.R., Lipzig, N.v., 2003. Response of wintertime Antarctic temperatures to the Antarctic Oscillation: results of a regional climate model. In: Domack, E., Leventer, A., Burnett, A., Bindschadler, R., Convey, P., Kirby, M. (Eds.), Antarctic Peninsula Climate Variability: Historical and Paleoenvironmental Perspectives, Antarctic Research Series 79. American Geophysical Union, Washington, DC, pp. 43–58.
Vaughan, D.G., Marshall, G.J., Connolley, W.M., Parkinson, C., Mulvaney, R., Hodgson, D.A., King, J.C., Pudsey, C.J., Turner, J., 2003. Recent rapid regional climate warming on the Antarctic Peninsula. Climatic Change 60, 243–274.
Venegas, S.A., Drinkwater, M.R., Schaffer, G., 2001. Coupled oscillations in Antarctic sea-ice and atmosphere in the South Pacific sector. Geophysical Research Letters 28 (17), 3301–3304.
Vernet, M., Martinson, D.G., Iannuzzi, R.A., Stammerjohn, S.E., Koslowski, W., Sines, K., Smith, R.C., Garibotti, I., 2008. Primary production within the sea ice zone west of the Antarctic Peninsula. Part I: sea ice, summer mixed layer and irradiance. Deep-Sea Research II, this issue [doi:10.1016/j.dsr2.2008.05.021].
White, W.B., Peterson, R.G., 1996. An Antarctic circumpolar wave in surface pressure, wind, temperature and sea-ice extent. Nature 380 (6576), 699–702.
Yuan, X., 2004. ENSO-related impacts on Antarctic sea ice: a synthesis of phenomenon and mechanisms. Antarctic Science 16 (4), 415–425.
Yuan, X., Martinson, D.G., 2000. Antarctic sea ice extent variability and its global connectivity. Journal of Climate 13 (10), 1697–1717.
Yuan, X., Martinson, D.G., 2001. The Antarctic Dipole and its predictability. Geophysical Research Letters 28 (18), 3609–3612.